NAVAL POSTGRADUATE SCHOOL

MONTEREY, CALIFORNIA

THESIS

DETECTION OF SUBPIXEL SUBMERGED MINE-LIKE TARGETS IN WORLDVIEW-2 MULTISPECTRAL IMAGERY

by

Michelle R. Sandersfeld

September 2012

Thesis Advisor: Richard C. Olsen
Second Reader: Charlene T. Sailer

Approved for public release; distribution is unlimited

THIS PAGE INTENTIONALLY LEFT BLANK

REPORT DOCUMENTATION PAGE		*Form Approved OMB No. 0704–0188*

Public reporting burden for this collection of information is estimated to average 1 hour per response, including the time for reviewing instruction, searching existing data sources, gathering and maintaining the data needed, and completing and reviewing the collection of information. Send comments regarding this burden estimate or any other aspect of this collection of information, including suggestions for reducing this burden, to Washington headquarters Services, Directorate for Information Operations and Reports, 1215 Jefferson Davis Highway, Suite 1204, Arlington, VA 22202–4302, and to the Office of Management and Budget, Paperwork Reduction Project (0704–0188) Washington DC 20503.

1. AGENCY USE ONLY *(Leave blank)*	2. REPORT DATE September 2012	3. REPORT TYPE AND DATES COVERED Master's Thesis
4. TITLE AND SUBTITLE Detection of Subpixel Submerged Mine-Like Targets in WorldView-2 Multispectral Imagery		5. FUNDING NUMBERS
6. AUTHOR(S) Michelle R. Sandersfeld		
7. PERFORMING ORGANIZATION NAME(S) AND ADDRESS(ES) Naval Postgraduate School Monterey, CA 93943–5000		8. PERFORMING ORGANIZATION REPORT NUMBER
9. SPONSORING /MONITORING AGENCY NAME(S) AND ADDRESS(ES) N/A		10. SPONSORING/MONITORING AGENCY REPORT NUMBER

11. SUPPLEMENTARY NOTES The views expressed in this thesis are those of the author and do not reflect the official policy or position of the Department of Defense or the U.S. Government. IRB Protocol number ___N/A____.

12a. DISTRIBUTION / AVAILABILITY STATEMENT Approved for public release; distribution is unlimited	12b. DISTRIBUTION CODE A

13. ABSTRACT (maximum 200 words)

The utility of satellite spectral imagery is analyzed for the detection of submerged mine like objects. The targets that were utilized were sub-meter in size and emplaced in the water off the coast of La Jolla, California for a barnacle study. There were three surface targets and three submerged targets that did not exceed three meters in depth. Two meter multispectral and half meter panchromatic WorldView-2 data were used for image processing and analysis.

The multispectral data proved more useful than the higher spatial resolution panchromatic data (sub-pixel vs resolved).For the multispectral data, principal component analysis was the most successful of the techniques, locating the submerged and surface targets. Attempts to use the RX-UTD anomaly detector were less successful, because of excessive false positives. This study supports the concept that commercial remote sensing is a viable option to support mine countermeasures.

14. SUBJECT TERMS Remote Sensing, Multispectral, Panchromatic, Mine Warfare			15. NUMBER OF PAGES 111
			16. PRICE CODE
17. SECURITY CLASSIFICATION OF REPORT Unclassified	18. SECURITY CLASSIFICATION OF THIS PAGE Unclassified	19. SECURITY CLASSIFICATION OF ABSTRACT Unclassified	20. LIMITATION OF ABSTRACT UU

NSN 7540–01–280–5500

Standard Form 298 (Rev. 8–98) Prescribed by ANSI Std. Z39.18

THIS PAGE INTENTIONALLY LEFT BLANK

**DETECTION OF SUBPIXEL SUBMERGED MINE-LIKE TARGETS
IN WORLDVIEW-2 MULTISPECTRAL IMAGERY**

Michelle R. Sandersfeld
Civilian, Department of the Navy
B.S., California State University at Monterey Bay, 2009

Submitted in partial fulfillment of the
requirements for the degree of

MASTER OF SCIENCE IN REMOTE SENSING INTELLIGENCE

from the

**NAVAL POSTGRADUATE SCHOOL
September 2012**

Author: Michelle R. Sandersfeld

Approved by: Richard C. Olsen
                 Thesis Advisor

                 Charlene T. Sailer
                 Second Reader

                 Dan Boger
                 Chair, Department of Information Science

iii

THIS PAGE INTENTIONALLY LEFT BLANK

ABSTRACT

The utility of satellite spectral imagery is analyzed for the detection of submerged mine like objects. The targets that were utilized were sub-meter in size and emplaced in the water off the coast of La Jolla, California for a barnacle study. There were three surface targets and three submerged targets that did not exceed three meters in depth. Two meter multispectral and half meter panchromatic WorldView-2 data were used for image processing and analysis.

The multispectral data proved more useful than the higher spatial resolution panchromatic data (sub-pixel vs. resolved).For the multispectral data, principal component analysis was the most successful of the techniques, locating the submerged and surface targets. Attempts to use the RX-UTD anomaly detector were less successful, because of excessive false positives. This study supports the concept that commercial remote sensing is a viable option to support mine countermeasures.

THIS PAGE INTENTIONALLY LEFT BLANK

TABLE OF CONTENTS

LIST OF FIGURES

LIST OF TABLES

THIS PAGE INTENTIONALLY LEFT BLANK

LIST OF ACRONYMS AND ABBREVIATIONS

AUV	autonomous underwater vehicle
DN	digital number
EOD	Explosive Ordinance Disposal
eV	electron volt
FWHM	full width half maximum
HSI	hyperspectral imagery
IED	improvised explosive device
ISR	intelligence surveillance & reconnaissance
J	joules
Km	Kilometers
m	Meters
m/s	meters per second
µm	Micrometer
MCM	mine countermeasures
MSI	multispectral imagery
ND	n-dimensional
nm	Nanometers
PC_1	first principal component
PC_2	second principal component
PCA	principal component analysis
REMUS	Remote Environmental Monitoring Units
ROC	receiver operating characteristic
ROI	region of interest
UAV	unmanned aerial vehicles
USMC	United States Marine Corps.
USN	United States Navy
UUVs	unmanned underwater vehicle
UWIED	underwater improvised explosive device

THIS PAGE INTENTIONALLY LEFT BLANK

ACKNOWLEDGMENTS

I would like to thank all of the people at the Naval Postgraduate School who have made this past year possible. Thank you to my professors and advisors for helping me get through this year in one piece. Thank you to the remote sensing staff for helping this program and our entire cohort get though its first year. Thank you to my classmates; we made a good team in helping each other complete this intense year together. Thank you to my fellow students who were working on this mine warfare project with me; our brainstorming sessions and your help throughout this thesis process were critical to my success. I would like to thank my friends and family for their patience with me being so scatter-brained this past year. Last but not least, I want to thank my boyfriend for his continued enthusiasm and support in my endeavors.

THIS PAGE INTENTIONALLY LEFT BLANK

I. INTRODUCTION

Naval mines have been and will continue to be a useful technique for coastal populations as a first line of defense. Since a majority of the world's population live relatively near the coast, coastal communities are important to consider when considering military strategy. Coastal areas are also vital in strategic planning when accessing a country from the sea or maintaining mobility in near shore waters. Naval mines can be a crucial tactic for forces to deny, slow down, or manipulate the movements of their enemy. Naval mines, or even the threat of, can give the psychological advantage to those laying them. Naval mines are a relatively cheap and easy to deploy and require the adversary to devote resources and time to clearing and securing an area.

Naval mines remain a real threat to the United States Navy (USN.). Since World War II (WWII) there have been four times as many USN ships seriously damaged or sunk by naval mines than all other types of attacks combined (Program Executive Office Littoral and Mine Warfare [PEOLMW], 2009). Throughout the history of the United States' involvement in naval mine warfare there has been an apparent cycle of the effort allocated. The focus of researching mine warfare happens when a conflict makes it absolutely necessary; then post conflict the budget begins to disappear and the perceived importance diminishes. Since naval mine warfare will continue to be a threat that enemies will continue to improvise and improve, it is critical that not only does the United States mine technologies continue to improve, but also the countermeasures progress. There are a variety of different technologies that are used in the mine countermeasure effort. Remote sensing technologies are becoming increasingly utilized for these efforts. For the purpose of this paper multispectral anomaly detection methods will be explored in order to determine if it is possible to locate naval mines. Data from the commercial WorldView-2 satellite will be utilized.

Countries around the world are contently devoting resources into developing more advanced naval mines. For this reason, it is essential the research also continue in the countermeasures of these weapons. Due to the danger that naval mines present to Explosive Ordinance Disposal (EOD) teams in locating and neutralizing mines, it is crucial that an effort be put into research and development of methods that allow naval mines to be remotely detected.

While the United States, like other countries, are developing more advanced technologies in mine warfare and countermeasures, it is important that current technologies be utilized to their fullest potential. There are many remote sensing platforms that are routinely collecting data; the problem is that the data is not always exploited to its full capability. Sometimes the data is not even exploited at all. With the current economic condition in the United States it is becoming even more important to insure that we are maximizing the use of the systems that are already in use. One thing to consider is if it is financially more responsible of the government to use commercial space platforms for their imagery data, rather than enduing the cost of developing and maintaining their own space systems.

The focus of this paper is to determine if it is possible to use the highest available resolution commercial space systems to locate both submerged and surface naval mines. It is a goal of this paper to determine if non-classified commercial data can be used to help with this mission. The use of non-classified data will allow for accessibility of the data to the warfighters on the ground, who need the data to help with their missions worldwide. Both multispectral and higher resolution panchromatic data will be used to try to reach this goal.

II.   BACKGROUND

Oceans have provided resources for human populations since early civilizations. A majority of the population can be found within a few hundred miles of the oceans (United States Marine Corps [USMC], 2009). Coastal waters around the world are extremely important to national security, growth and prosperity (Borden, 2000). The close proximity of the oceans have helped fuel a variety of endeavors including: trade, food, travel, and military actions. As the world's population continues to increase, it is estimated that the littoral zones will be even more heavily concentrated. As coastal communities become more populated it becomes even more critical that techniques are in place for military operations in the ever-changing, difficult to access littoral zone. The littoral zone consists of not only the seaward portion, which is from open ocean to the shoreline, but also the landward portion, which is the land that can be directly protected and supported from the ocean (USMC, 2009). These coastal zones around the world are dynamic in nature, with changes happening in a matter of hours in some cases. Therefore, frequent monitoring is required for successful military operations in these coastal zones. When it comes to naval operations, the littoral zones are considered extremely important (Holland et al., 2002). For the USN and USMC the littoral zone can provide critical entry points for assaults or extractions, maneuvering space, ability to respond to crisis situations, as well as accessibility for countermeasures to any enemy tactics in the littoral zones (USMC, 2009).

For centuries, there has been interest in exploring the unknown world of our oceans. There have been a number of technological advances that have aided in both exploration and monitoring, including but not limited to: underwater flashlights, underwater cameras, diving equipment, glass bottom boats, submarines, remotely operated vehicles (ROVs), autonomous underwater vehicles (AUV), sonars, multispectral, and hyperspectral scanning systems. It is becoming increasingly important to continue improving upon these technologies

3

for not only environmental monitoring and research, but also for homeland security. Due to the naval mine warfare tactics expected to be used in future conflicts, it remains important for the development of techniques that will adapt to these challenges while continuing to keep both the warfighter and civilians safe.

Naval mines and underwater improvised explosive devices (UWIEDs) have been, and continue to be, an issue that the United States has to face in coastal zones all over the world, making it important to continue to improve the technologies that will help counter naval mines and UWIEDs. In order to keep troops safe it is crucial that military leaders in coastal areas can make use of the tools that are available to identify and locate naval mines/UWIEDs. It is essential that the United States countermeasure technology continue to improve to keep up with the ever-changing naval mines/UWIEDs.

Naval mines or UWIEDs can be a first line of defense for coastal countries; used to deny, slow down, or manipulate movement of the enemy. Mine warfare can be an important aspect of sea control. The forces who are laying the mines also get the psychological advantage created by the threat of the explosives. Naval mines/UWIED force the enemy to put resources and time towards clearing the mines, potentially leaving forces vulnerable to attack. Naval mines/UWIEDs are relatively easy and cheap to deploy. The time it takes to clear mines is two hundred times greater than that which it takes to lay the mines (Khan, 2010).

The line between traditional naval warfare and terrorists using improvised devises is becoming blurred; the Secretary of Defense had described this as "hybrid wars" (PEOLMW, 2009). Forms of improvised explosive devices are used both on land and underwater. As stated in Joint Publication 3-07.2 *Antiterrorism* (2010), an IED is "a device placed or fabricated in an improvised manner incorporating destructive, lethal, noxious, pyrotechnic, or incendiary chemicals and designed to destroy, incapacitate, harass, or distract" (p. II-14). Based on this definition of IEDs, some of the naval mines that have been used have characteristics that fall under the IED category, and can have the same dramatic

4

effects as traditional naval mines. For this reason, throughout this report the terms naval mines and UWIEDs may be generalized into one category

A.   TYPES OF NAVAL MINES

There is a large variability between naval mines/UWIEDs. There are an assortment of devises that can be further modified depending on the intended targets. For example they can be deployed at depths ranging from less than 10 to over 200 feet; and the charge can range anywhere from a few pounds to several tons. Although there are many forms and configurations for naval mines/UWIED they can be simplified into four primary groups: drifting mines, moored mine, bottom or "ground" mines, and limpet mines (PEOLMW, 2009).

1.   Drifting Mines

Drifting mines are the simplest, easiest to deploy and counter, form of naval mines. Drifting mines/UWIEDs are positively or neutrally buoyant and are carried by the tides or currents. Some drifting mines, known as oscillating mines are designed so they will move between two desired depths, making them even more hazardous. Drifting mines are internationally banned, although remain in use, because they do not follow the international treaty requirement that mines must become inactive within an hour of detachment from an anchor (PEOLMW, 2009; Khan, 2010).
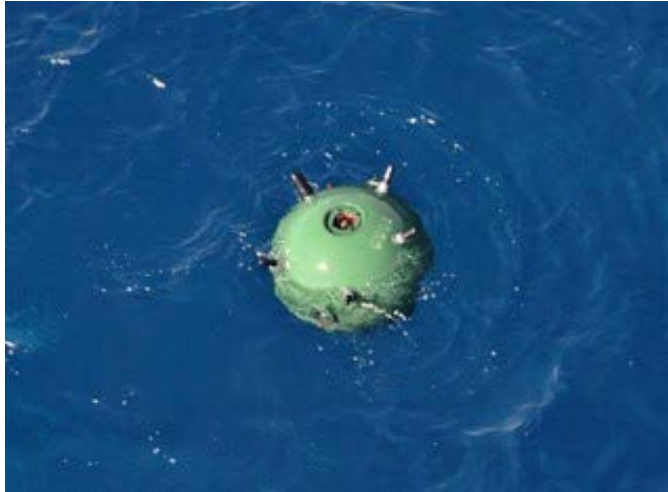
Figure 1.   Drifting Mine
This image shows an example of a drifting mine in the water (From Allied Joint Force Command Naples [AJFCN], 2012).

2.   Moored Mines

Moored mines tend to be more technologically advanced than drifting mines. These mines carry smaller charges due to the limitation of space within the mine, due to the large air pocket required to keep them floating at the desired depths. Detecting moored mines is more difficult than drifting mines (Khan, 2010). There are several sub-categories of moored mines/UWIED: near-surface mines, in-volume mines, and close-tethered mines that remain near the seafloor. A dangerous variation of moored mines are rising mines, which shoot a rocket propelled projectile into the enemy target, increasing the mines "reach" and ability to cause damage (Khan, 2010; PEOLMW, 2009). Figure 2 depicts how one of these rising mines attacks an enemy vessel.

A. MINE CASE
B. MINE CASE COVER
C. TRIPPING AND FIRING MECHANISM
D. MINE CHARGE
E. ANCHOR
F. DISTANCE WEIGHT
G. MOORING CABLE
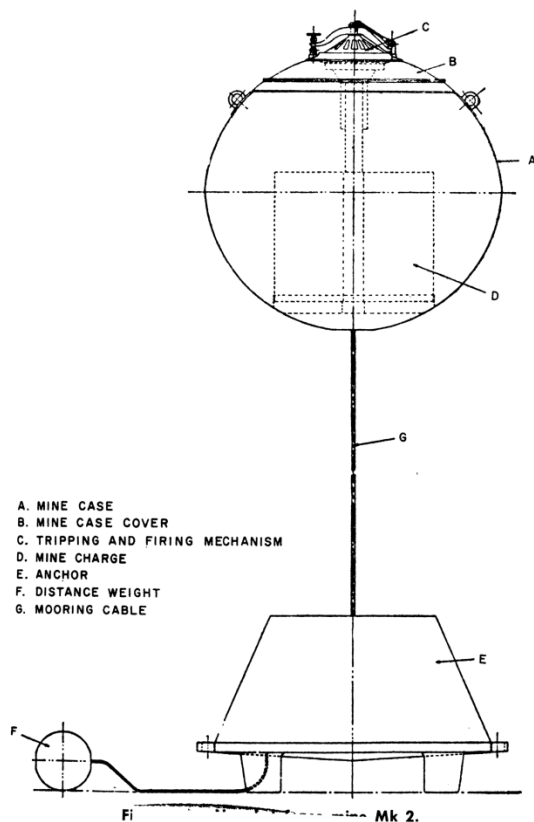
Naval Defense Mine Mk 2
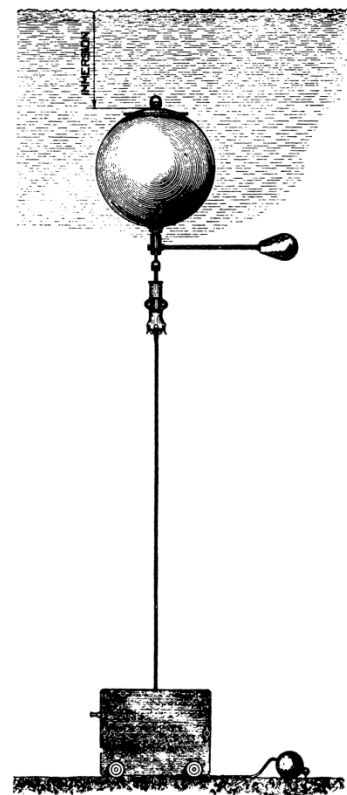
Naval Defense Mine Mk 3

Figure 2.   Moored Mine

Drawings are from Minemen (1997) and shows a moored mine that would be found under the surface of the water (p. 25). Moored mines can also have long enough cable that the mines can be floating on the surface.
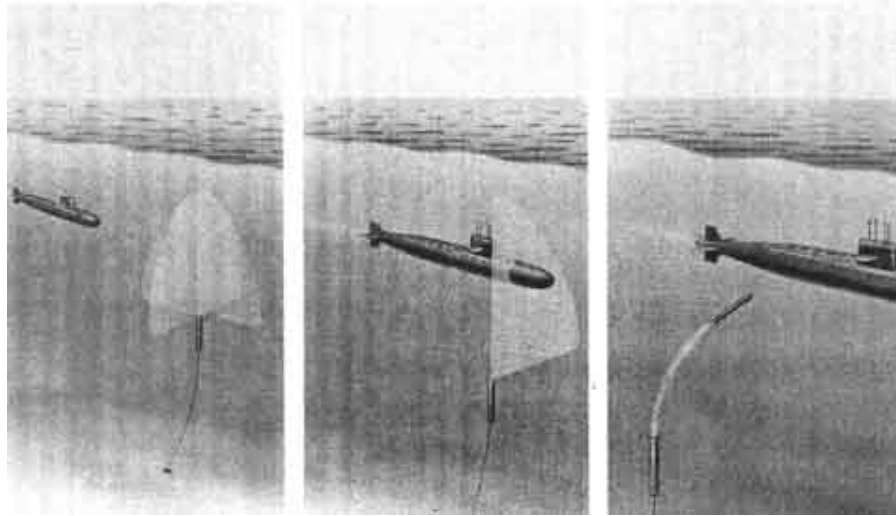
Figure 3.   Rising Mine

This drawing illustrates how a moored rising mine detects and detonates when a submarine or surface ship passes (From Shirokorad, 2009).

3.   Bottom or "Ground" Mines

Bottom mines are the largest naval mines/UWIEDs in both physical size and capacity of explosive charge (upwards of 1.5 tons). Bottom mines rest on the seafloor and are held in place by their own weight. Their shape can vary anywhere from a 36-inch cone to a 12-foot-long mine. The limiting factor of bottom mines is the water depth. These mines must release enough energy to travel though the water column and still create damage to the enemy ship, making them inefficient in deep water for surface targets. Bottom mines are, however, effective in deeper water against submarines (Khan, 2010; PEOLMW, 2009).
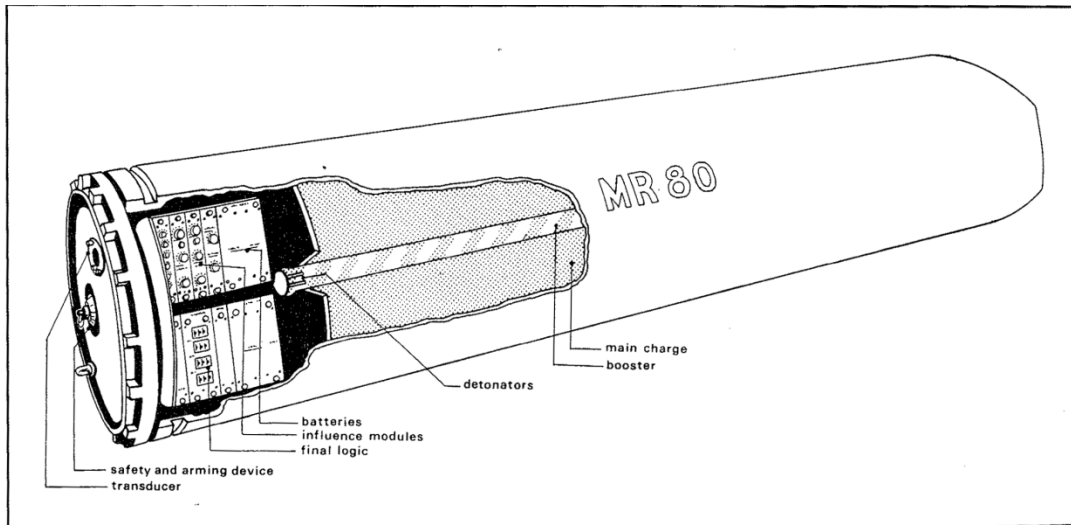
Figure 4.   Bottom Mines

This figure, from Watts (2005), shows and example of an influence bottom mine (p. 350).

4.   Limpet Mines

Limpet mines are used as a direct attack on a specific target. They are attached to the hull of targeted ships by human divers. The explosion of a limpet mine can be programed to take place after placement, with the timeframe varying anywhere from minutes to days, or even longer (PEOLMW, 2009).

Figure 5.   Limpet Mines
This image, from Watts (2005), shows an example of a limpet mine that can be placed on a hull of a ship (p. 356).

B.   DETONATION AND DEPLOYMENT

Naval mines/UWIEDs are designed to detonate three different ways: contact, command-detonation, or in the presence of "influences" or signatures given off by ships or submarines. Contact mines are the oldest mine method still in use, and can take the form of either drifting or moored mines. The most common method of triggering contact mines is to have a vial of chemicals within a horn on the outside of the mine, which when broken serves as a catalyst for the detonator. Command-detonation mines are either bottom or moored mines that are detonated by an individual when the enemy ship reaches the desired location. These mines tend to be limited to harbors and restricted waterways, and used as a method of defensive movements. Mines that detonate when a signal is received from a ship or submarine are called influence mines. Influence mines are either moored or bottom mines, and contain technically advanced sensors and firing mechanisms. Influence mines can have either a solitary or combination of sensors, which can be magnetic, acoustic, seismic, pressure or underwater electrical potential detectors (PEOLMW, 2009).

10

Naval mine technology has greatly improved over the decades. Modern naval mines are becoming so sophisticated that they use microcomputers which have the ability to not only detect a target, but determine if it is a ship or a mine sweeper and are able to resolve the ideal time to detonate as the vessel passes. More strategy and creativity is going into the mines that are being manufactured. Naval mines/UWIEDs are becoming harder to detect and more of a potential problem. For instance, naval mines are being designed using plastic and fiberglass, or fitted with influence sensors making them tremendously challenging to detect, identify, or counter (PEOLMW, 2009; Khan, 2010).

Naval mines are no longer just standardized war elements; countries are improvising their uses and deployment methods. Naval mines of past eras are now being retrofitted with sophisticated modern mechanisms and counter-countermeasure features. Placement can be done using surface ships, aircraft, pleasure boats, submarines, combat divers, or even pushing them off the back of pickup trucks as they cross over bridges (PEOLMW, 2009). Iran for example uses unconventional platforms such as small speedboats, open-decked ships, and disguised merchant vessels. The advantage of using these platforms are they are agile, challenging to detect, inexpensive, and as they are so numerous it allows for the number of useable platforms to be increased as the need arises. There are disadvantages for the user of these platforms as well: they have limited operating ranges, only light armoring, limited weapons loads, and have to be in close vicinity of enemies with whom they wish to engage. The staging areas for these missions are becoming less predictable, as it is no longer just the coastal bases being used, they now include nearby islands and offshore oil rigs (Khan, 2010).

C.   HISTORY OF MINE WARFARE

The idea of naval mines or UWIEDs actually dates back to 673, when Constantinople was defended with "Greek Fire." The United States has used naval mines/UWIEDs and their countermeasures in a number of wars and conflicts over the last 230 years that include the Civil War, Spanish-American

War, World War I and II, Korea, Cold War, Operation Desert Storm and Operation Iraqi Freedom (PEOLMW, 2009). The use of naval mines by the United States have resulted in mixed success; failures were primarily due to the lack of countermeasures.

1.   1700s and 1800s

The first American attempt at naval mines (then called torpedoes) was unsuccessful, and took place in 1776 in the Hudson River against the *HMS Eagle*. Success using naval mines/UWIED first occurred for the United States during the War of 1812, when naval mines effectively kept the British from entering the Port of New York. During the Civil War, naval mines were an important strategy for the South, resulting in 48 severely damaged or sunk Union ships (PEOLMW, 2009). In 1862 during the Civil War, was the first recorded event of the United States using mine warfare countermeasures. The Union Army used rafts with hooks that would "catch" the mine's mooring lines (Borden, 2000). During the Spanish-American War the United States had to deal with naval mines in both Manila Bay and Santiago (PEOLMW, 2009).

2.   World War I and II

In 1917, the United States was entering World War I (WWI) with the same level of naval mine capabilities as at the end of the Civil War; all mines were moored contact mines (Borden, 2000). During WWI, thousands of naval mines were laid for strategic sea access denial (PEOLMW, 2009). Countermeasures used in WWI consisted of dragging a cable behind ships, sweeping for mines. This method was used extensively after the war to clear the North Sea Barrage, which was a large minefield laid by the United States and allies during WWI between the Orkney Islands and Norway. After WWI the United States appeared to understand the importance of developing mines, mine laying, and minesweeping techniques. In 1919, at the Washington Navy Yard, a "Mine Building" was established for physicists, engineers, and draftsmen. In 1929, this group was incorporated into the Bureau of Ordnance, part of the Naval Ordnance

Laboratory. The funding for this group was lost, and therefore the progress remained slow. For this reason the United States capabilities, entering WWII were not much further along than they had been twenty years before. Meanwhile, the naval mines of other countries had significantly advanced (Borden, 2000).

A variety of naval mines were used in WWII, both in the United States waters and abroad. In 1945, during a 6-month time span, 25,000 mines were laid by USN and U.S. Army in Japanese waters (including shipping routes). This operation resulted in Japan losing maritime commerce, and 760 ships with many more ships damaged (PEOLMW, 2009). During the war, Germans began deploying newly developed bottom mines that utilized magnetic sensors. It became a scramble for the United States and their allies to develop a magnetic sweep to counter this new technology. Mine warfare technology continued to advance, and by the end of the war, mines were advanced enough that they could require a combination of magnetic, acoustic, and pressure signatures from a vessel in order to detonate (Borden, 2000).

3.   Korean Conflict

The Korean Conflict is an example in which the United States naval mine countermeasures failed. Going into the Korean Conflict, the United States believed that with the atomic age and the use of extensive air defense having become common practice, offensive minefields would be impossible and defensive minefields obsolete. Due to the unanticipated minefields, operations were delayed for weeks (Borden, 2000). Naval mines placed by the Korean force caused damage to 11 United States warships during the conflict (Khan, 2010). Of the 500 mine clearance ships the United States had after WWII there were only 15 left by the summer of 1950. While only two percent of all United Nations naval service members made up the mine countermeasures force, they made up 20 percent of United Nations naval causalities during the Korean Conflict (PEOLMW, 2009). After the Korean Conflict, the USN gave naval mines a higher

priority. Into the 1950s and 1960s the Mine Defense Laboratory continued research in minesweeping, mine hunting, mine classification and mine neutralization (Borden, 2000).

4. Vietnam War

During the Vietnam War the United States once again showed success in both the use of naval mines/UWIED and countermeasures. Using aircraft the United States improvised 11,000 general-purpose bombs, and dropped these "destructor" mines into coastal and inland waterways. Later in the war, thousands more mines were planted halting all water-borne trade with North Vietnam (PEOLMW, 2009). After the Vietnam War, during Operation End Sweep the latest techniques were used to clear the minefields that had been laid during the war (Borden, 2000).

By the end of the 1970s the United States mine countermeasure capabilities were declining. At this time the mine countermeasure resources were made up of 21 helicopters and 21 wooden hulled minesweepers (18 of which were reserve), all of which were built in the early 1950s or before. The only new addition during this time was the mine hunting sonar installed on the helicopters. The aging helicopters and minesweepers were again used in 1987 for clearing mines in the Arabian Gulf. It was not until the late 1980s that the Vietnam War era helicopters were replaced, but the same minesweeping and mine hunting systems remained in use on these new helicopters (Borden, 2000).

5. Middle Eastern Conflicts

In the past 20 years the United States has had both success and failures in countering the use of naval mines/UWIEDs in the Middle East. In 1988 at the end of the Tanker War in the Arabian Gulf, the United States had $96 million of damages to the USS Samuel B. Roberts, caused by a $1,500 Iranian contact mine (Khan, 2010; PEOLMW, 2009). In the early 1990s during Desert Shield and Desert Storm, the United States was once again under-prepared for mine warfare and confirmed the importance of integrating mine countermeasures

within the deployed fleets (Borden, 2000). In the Northern Arabian Gulf during Desert Storm, Iraqis laid an assortment of 1,300 naval mines consisting of both WWII era mines and a newly designed multiple-influence mine. The result of these mines was serious damage to both the USS *Tripoli* (LPH-10) and the USS *Princeton* (CG-59), as well as halting a planned amphibious assault. The Gulf War was the last combat in which the USN laid naval mines (PEOLMW, 2009).

In 2003, during Operation Iraqi Freedom, United States intelligence, surveillance, and reconnaissance (ISR) assets determined that Baghdad was likely to attempt to plant naval mines in the Northern Gulf. Due to this intelligence, special operation teams successfully captured disguised Iraqi "mine layers" with over 100 mines on-board (PEOLMW, 2009). Due to the nature of naval mines, the threat does not cease to exist because there has been an official end of conflicts. This was seen after the end of the First Gulf War when Iraqi mines damaged two United States warships (Khan, 2010). There are many man-hours and resources required before an area planted with naval mines/UWIEDs can once again be considered safe.

6.   Past Challenges and the Mine Warfare Cycle

Throughout history it has been a challenge to adjust countermeasures to meet the demands of new naval mine technology. While at the same time, new naval mines and methods to counter current countermeasures must be developed. Another challenge is that the success of a countermeasure technique varies between locations and situations. The efforts of clearing naval mines is often slowed by the fact that mine countermeasure resources are not readily available in the needed region, as they are expensive and vulnerable assets (Khan, 2010).

Based on previous history there is an apparent cycle when it comes to mine warfare. The United States puts the effort into mine warfare during or right after a conflict and then loses interest, leaving our country at a disadvantage when the next battle arises. Figure 6 from Borden (2000), shows the cycle that the USN has fallen into the past.

15
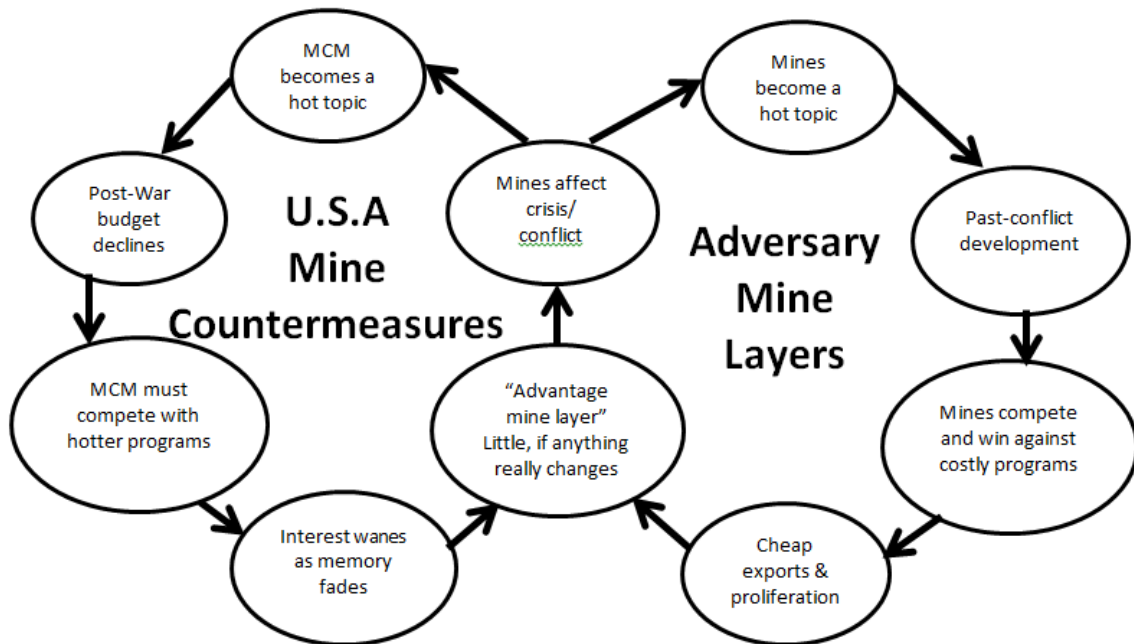
Figure 6.   Mine Warfare Cycle
This flow chart, from Borden (2000), shows the mine warfare cycle representing past wars and the subsequent peace times.

D.   COUNTERMEASURES

In the past naval mines have not been given the priority required to be effectively countered, only to become a huge concern as conflicts arise (Rabiroff, 2011). Naval mines/UWIEDs are becoming harder to detect and more of a potential problem. Some of the aspects that can make locating mines today difficult include: unconventional case design, sonar deflecting paneling, non-metallic construction, and self-burying features (Gilbert, 2001). More strategy and creativity is going into mine development, requiring the countermeasures to also continue to improve.

1.   Methods of Clearing Mine Fields

The process of locating and clearing naval mines has been a complex one that contains many aspects. Figure 7 shows the many different aspects of mine countermeasures. Some of the variety of countermeasure methods that have

been used include degaussing of major ships, paravanes, an assortment of mechanical/magnetic/acoustic sweeping technologies, marine mammals, and air assets (blimps & helicopters) dedicated to naval mine warfare. As naval mines become more complex traditional minesweeping methods become ineffective leaving forces to revert to more time-consuming strategies such as unmanned underwater vehicles (UUVs) and human divers. High frequency sonars, unmanned aerial vehicles (UAV), and UUVs are frequently relied on to gather intelligence about naval mines (Khan, 2010; PEOLMW, 2009). Figure 8 shows an autonomous underwater vehicle (AUV) that is used to locate naval mines.
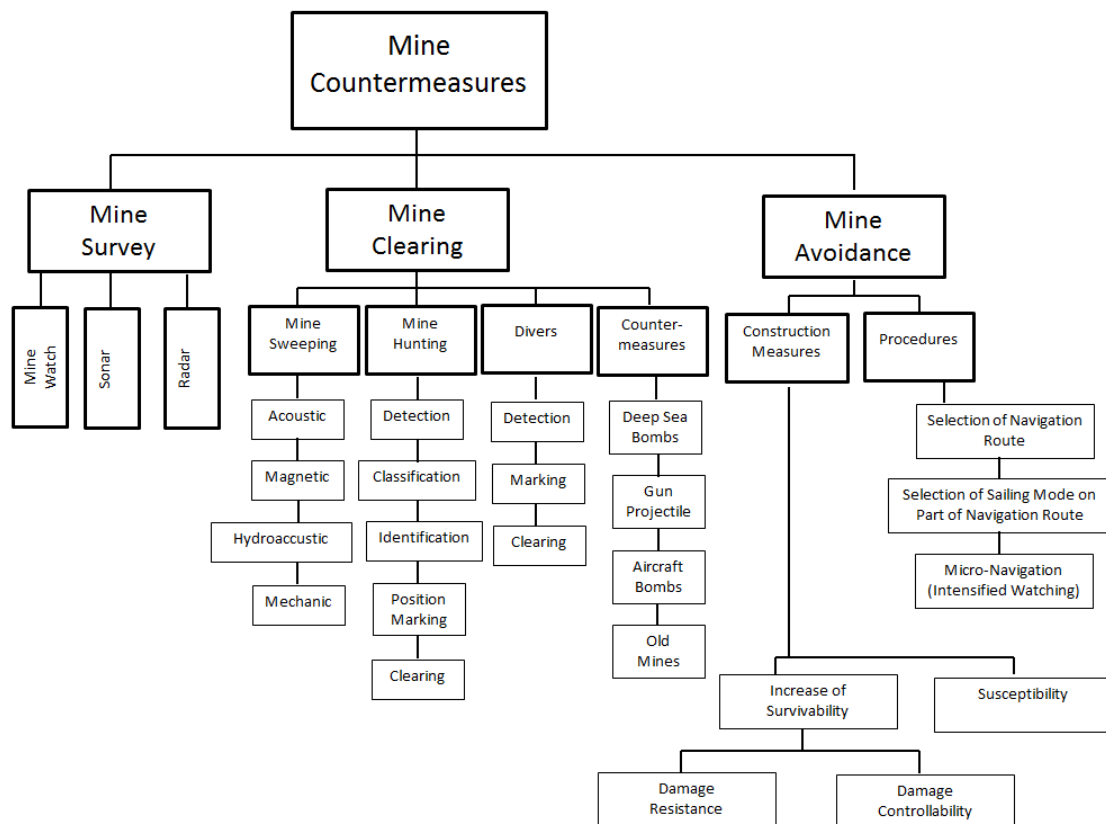
Figure 7.   Countermeasures of Mine Warfare
This chart from Matika and Koroman (2001) shows the many different elements of mine countermeasures
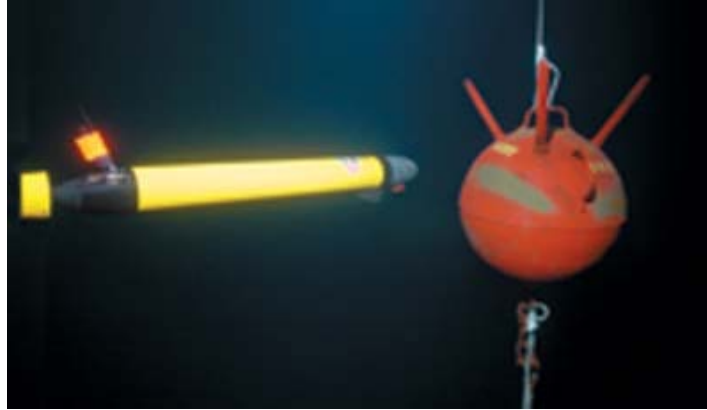
Figure 8.   AUV Locating Mine

This is an example of an AUV that is used to locate naval mines. The AUV showen above is known as a Remote Environmental Monitoring Units (REMUS). The REMUS was used for wide area surveys and reconaissance of waters up to 100 meters deep during the invasion of Iraq in 2004 (From Whitford, 2005).

Mine countermeasures are split into two types of procedures: minesweeping and mine hunting. Minesweeping methods are used when there is a known mine or minefield. Mine hunting methods are used when the mine or minefield is unknown (Matika & Koroman, 2001).   Most naval mine countermeasure platforms include equipment for both mine hunting and minesweeping (PEOLMW, 2009). The vessels currently in use fail to offer a complete solution for clearing naval mines, as they cannot address mines found in shallow water or the surf zone. Currently these shallow areas must be addressed with the limited capabilities of marine mammals and UUVs (USMC, 2009).

Mine hunting consists of five steps: detection, classification, localization, identification, and neutralization. Using these steps can offer a reasonably large level of certainty that the risk of naval mines in a particular area is diminished. There are two kinds of minesweeping systems: influence and mechanical. In influence minesweeping the mines are set off by mimicking the signatures of a ship that is the catalyst for mine detonation. For mechanical sweeping the method is either to physically damage the mine (i.e., cutting control wires), or

cutting the tether and then neutralizing the mine (PEOLMW, 2009). Mine clearing is dangerous and can take a lot of time and resources, both during and long after the conflict.

2. Historic Mine Clearing Examples

There have been several examples throughout history where major naval minesweeping efforts have taken place. After WWII there was a major effort to retrieve the naval mines that the United States laid in Japanese water, taking hundreds of vessels several years. Despite the massive effort, in 1971 the USN estimated that there were still more than 2,000 sensitive influence mines that were never found. After Desert Storm it took the United State and coalition forces several years to clear the mines and declare primary water ways safe for ship traffic (PEOLMW, 2009).

E. A FUTURE WITH NAVAL MINES

Due to the variability, adaptability, and need for ever-changing countermeasures, naval mines present a potentially serious threat to the world today. Since WWII there have been four times as many USN ships sunk or seriously damaged by naval mines than all other forms of attack combined (PEOLMW, 2009). Although many Americans don't realize it, the threat of mines/UWIED will remain a serious concern for United States security in future conflicts and terrorist attacks. The fact that naval mines are cheap, easy to deploy and can cause massive amounts of damage make them a desirable weapon for many countries and terrorist groups.

Naval mines/UWIEDs can be used as a nuisance or to create a larger disaster, with a variety of goals including political, economic, military ends, or psychological effects. Since 90 percent of all imports and exports travel though our ports, an attack on our country's ports and waterways could have devastating effects (PEOLMW, 2009). A major attack on our waterways could have a severe economic effect on not only the United States but also on economies worldwide. This is one of the many reasons it remains important for the United States to

continue to improve naval mine counter measures capabilities for the wide variety of ever-changing naval mines.

When looking at the surpluses of naval mines around the world it is clear that naval mines/UWIEDs need to be treated as a serious threat, and considered in the security of this country. In 2009, it was reported by the USN that there are 50 different countries with 300 different varieties of naval mines. There are more than thirty countries around the world that produce naval mines, more than twenty of which will export them. Excluding United States weapons and anything classified as an UWIED, it was reported that there is a worldwide surplus of a quarter million naval mines (PEOLMW, 2009).

1. Threats to Consider

When it comes to naval mines/UWIEDs in today's world there are a variety of threats the United States must consider. Iranian mines are ten times as powerful as those used in the Tanker War (Khan, 2010). China reportedly has 80,000 naval mines prepared to deploy if any potential conflict arises. North Korea reportedly has nuclear naval mines, with the intention to use them to counteract any advantage the United States and or other country's forces could have over them in a conflict (Rabiroff, 2011).

Since naval mines/UWIEDs are a threat that will be present in the future, new techniques to counter them are needed. The method under consideration for this paper is the use of remote sensing, in particular multispectral imagery, to locate naval mines. There is a range of platforms that could be utilized; for this paper the remote sensing satellite WorldView-2 will be examined.

F. REMOTE SENSING

Remote sensing has become a common technology used to examine problems ranging in scale from small to large, both in the government and civilian industries. There are both active and passive remote sensing technologies. The active systems emit their own energy, which is measured upon return; these systems include radar, lidar, and sonar. The passive systems include thermal,

hyperspectral, and multispectral imaging. Sensors that collect data passively measure the electromagnetic radiation that is reflected or emitted from the surface. Changes in atmosphere, ground conditions, scene temperature, solar illumination, and sensor response can all dramatically affect the radiance detected by the sensor (Mayer & Bucholtz, 2003). As technologies improve, the finer scale problems will be more accessible for study with increased accuracy.

Hyperspectral, and to a lesser degree, multispectral products can provide analysts with a spectrum that can help differentiate between materials. While there are a variety of bands on many of the sensors, the optimum band(s) to use for analysis depend on the mission goals. There are a number of spectral sensors on satellites and airborne platforms that collect varying numbers of bands of data with varying spectral, spatial, and radiometric resolutions.

Remote sensing imagery provides analysts with a multitude of intelligence. These technologies have been widely used in terrestrial settings, and are becoming more common to look at features under the ocean, providing further value to these systems. Bathymetric and coastal measurements can be important for environmental planning, marine navigation, military operations, trade, and the travel industry; as coastal environments are such a dynamic, ever-changing environment. Currently remote sensing is a resource the United States government is exploiting and further developing towards mission goals such as countering naval mines/UWIED.

1.   Electromagnetic Energy

Many remote sensing studies are centered on finding a relationship, between the level of electromagnetic energy that is either reflected, emitted, or backscattered in particular bands, and the phenomena characteristics that are being researched. While the majority of the electromagnetic energy recorded in passive sensors is from the sun; all objects with temperatures above absolute zero will emit some level of electromagnetic energy (Jensen, 2005). Electromagnetic energy is emitted or absorbed in units called photons

(Campbell, 2007). The level of energy emitted from an object is a function of its temperature; and therefore the sun will emit far more energy than the earth, as shown in Figure 9 (Jensen, 2005).
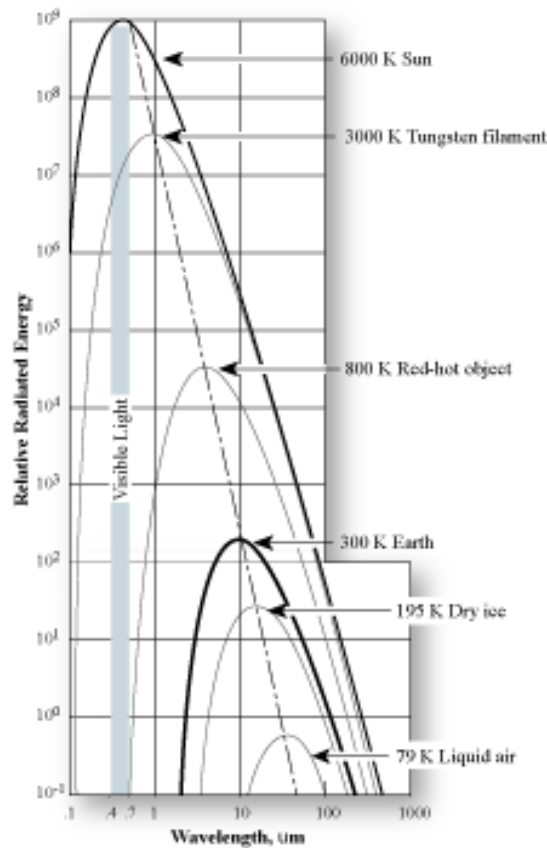
Figure 9.   Radiation Curves

The figure above shows how radiant energy varies with the temperature of the object (From Jensen, 2005).

While visible light is what we, as humans, can see, it makes up only a small portion of the electromagnetic spectrum. The sun produces a continuous spectrum of electromagnetic radiation from gamma rays to radio waves, however the dominant wavelength is 0.48 micrometers (µm), (Figure 10). Approximately, 41% of the energy produced by the sun is found in the visible spectrum, between 0.4 and 0.7 µm (Jensen, 2005). It is also common to describe electromagnetic energy as electron volts (eV) and photon energy units known as joules (J), (Figure 11) for visible light.

22
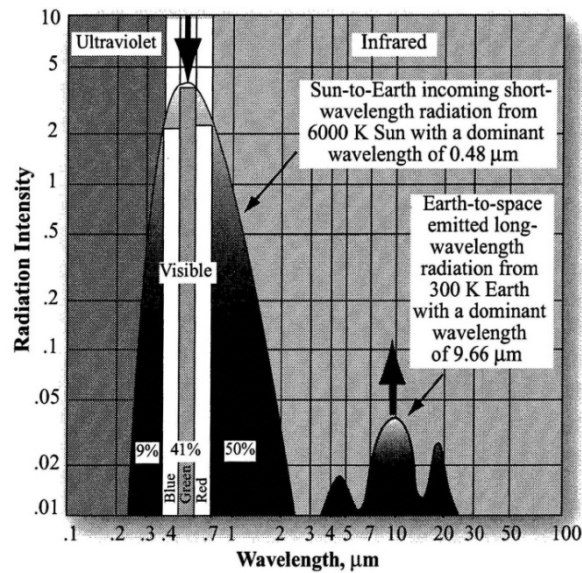
Figure 10.   Wavelengths Produced by the Sun
This figure illustrates the concept that the majority of energy produced by the sun
center around 0.48 µm (From Jensen, 2005).
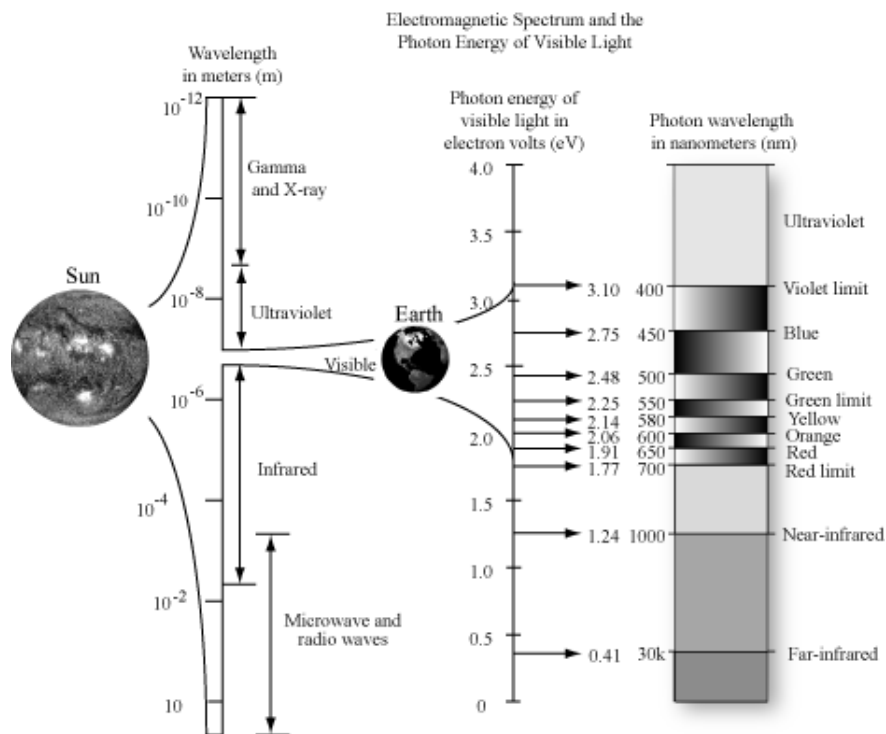
Figure 11.   Photon Energy of Visible Light
The relationship between wavelength and eV of electromagnetic energy is shown
in the above figure (From Jensen, 2005).

Electromagnetic radiation is the form of energy transfer used in remote sensing due to the fact that it is the only type of energy transform that can take place in a vacuum, and can therefore take place in space. Electromagnetic radiation takes place whenever an electrical charge is accelerated or decelerated. The length of time that the charged particle is accelerated dictates the wavelength and the number of accelerations that take place in a second determines the frequency. The shorter the wavelength the higher the frequency will be, as wavelength and frequency are inversely proportional. As electromagnetic radiation moves between substrates, the frequency will remain the same, while the speed and wavelength will alter (Jensen, 2005).

The electromagnetic energy produced by the sun travels through space at the speed of light (3×10^8 meters per second). This energy interacts with the Earth's atmosphere and then again with Earth's surface. Interacting with the Earth's atmosphere can affect the speed, wavelength, intensity and spectral distribution of the radiated energy (Jensen, 2005). The atmosphere becomes even more of a problem with space-based platforms then airborne platforms as the energy must travel further.

2. Reflectance, Scattering, and Absorption

When interacting with Earth's atmosphere, or surface, there are several interactions that take place, including: reflectance, scattering, and absorption. The result of these processes can greatly reduce the amount of radiation hitting the target. The radiation that returns to the sensor is even further reduced, as after hitting the target as it must travel again though the atmosphere on its way back to the sensor.

Reflection is the process of radiation bouncing off a nontransparent surface in a predictable direction. The size of the surface irregularities in relation to the wavelength of the radiation plays a role in the reflection (Campbell, 2007). There are several types of reflection: specular, near-perfect specular, Lambertian and near perfect diffuse reflection. Specular reflection takes place when the surface hit by the energy is smooth and a near-perfect specular reflector

happens when the surface is almost smooth. For both of these examples the energy will reflect at an equal and opposite angle, with the only difference being that in the near-perfect specular reflector a small amount of light will reflect at other angles. Lambertian is another name for a perfect diffuse reflector, which happens when the radiant energy is diffused but equal at any angle. The last type of reflection is near-perfect diffuse; the resulting reflection is fairly predictable but not equal in all directions (Jensen, 2005).

Scattering is where the light bounces off something in an unpredictable direction. There are three types of scattering: Rayleigh, Mie, and nonselective. Rayleigh scattering is also known as molecular scattering, and takes place when the diameter of the matter (such as air molecules) is much smaller than the electromagnetic radiation wavelength. A majority of the Rayleigh scattering that is due to gas molecules, takes place between two and eight kilometers (km) above the ground. Mie scattering is also known as non-molecular or aerosol particle scattering and happens when the particles have a diameter roughly the size of the electromagnetic radiation wavelength. Mie scattering tends to occur in the lowest 4.5 km of the atmosphere. Dust and smoke are examples of mediums that results in Mie scattering in the visible spectrum. Mie scattering tends to be greater and has longer wavelengths then Rayleigh scattering. The final kind of scattering, known as nonselective scattering occurs in the lowest portion of the atmosphere where the particles are greater than ten times the radiation wavelength. Unlike the other types of scattering, where parts of the spectrum are more affected, in the nonselective all wavelengths are scattered. The ice crystals and water droplets making up fog and clouds are an example of nonselective scattering sources because all colors are scattered the fog and clouds appear white (Jensen, 2005).

Absorption takes place when the atmosphere prevents radiation from being transmitted (Campbell, 2007). Absorption is a process where the radiant energy is absorbed and then changed into some other form of energy (Jensen, 2005). Absorption becomes an important aspect to understand and optimize

remote sensing technologies. The three gases that cause most of the absorption of solar energy are ozone, carbon dioxide and, water vapor (Campbell, 2007). In the electromagnetic spectrum there are ranges of wavelengths, called absorption bands, in which radiant energy is absorbed by a particular substance (Jensen, 2005). The absorption bands of common components of the atmosphere are shown in Figure 12.
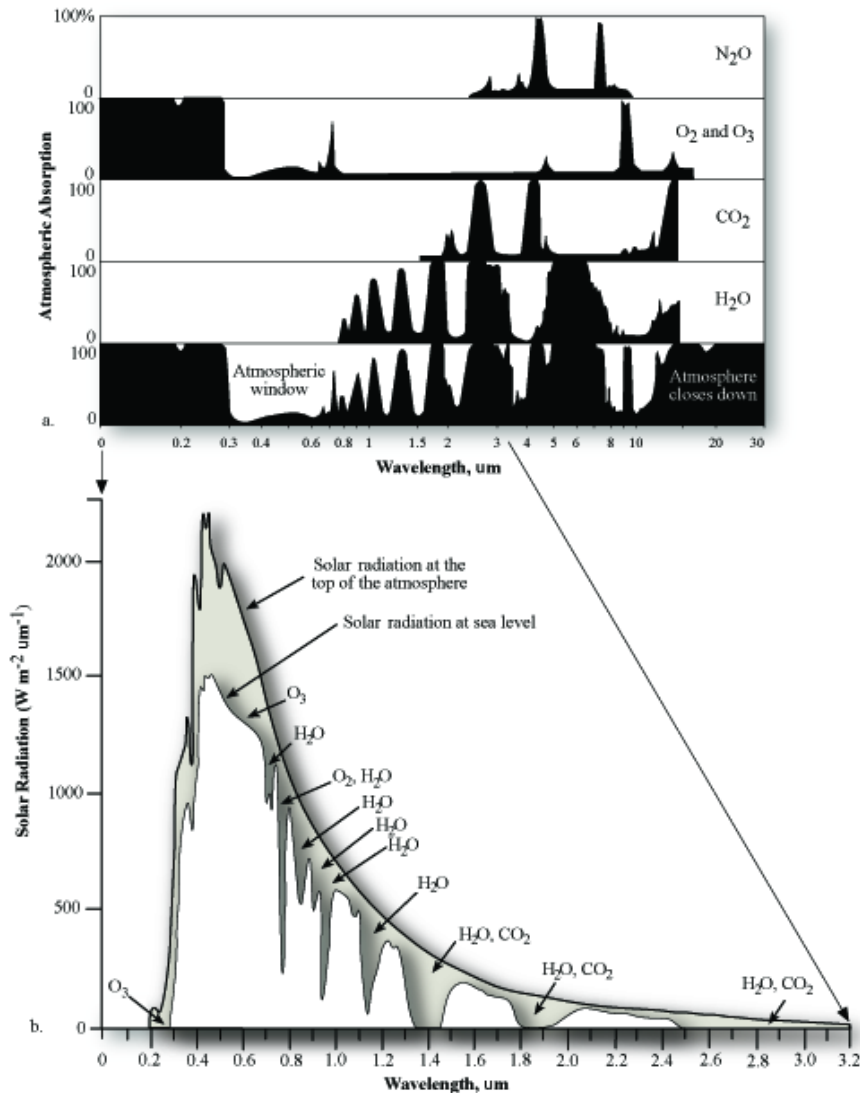

Figure 12.   Absorption Bands

Gases in the atmosphere have different absorption bands. The bottom part of the figure shows how the effects of the atmospheric scattering, absorption, and reflectance combined and the solar energy-reaching sea level is reduced (From Jensen, 2005).

Knowledge of these atmospheric absorption bands is important for remote sensing as the absorption in the atmosphere can mean that the sensor may not detect the energy from the target it is trying to measure. Remote sensing of the ground needs to take place in atmospheric windows, which is an area where particular wavelengths are easily transmitted though the atmosphere. The absorption spectra of the atmospheric gases are responsible for determining the position, extent, and effectiveness of atmospheric windows (Campbell, 2007). Certain wavelengths are affected much less by scattering than by absorption. This is the case in wavelengths shorter than the visible spectrum and in the infrared spectrum (Jensen, 2005).

3. Radiance

Radiance and reflectance are two common attributes to examine when analyzing passive remote sensing data. Radiance is the data collected from the sensor and reflectance is in turn calculated. Radiance measures the intensity of the energy that is reflected from the surface. The defining factors of radiance are wavelength, spatial area (angle), and intensity (Campbell, 2007). Radiance is the most precise radiometric measurement in remote sensing. Radiance is an approximate measurement of the radiant intensity per unit of the area measured in a specific direction. There could be radiance leaving an object in multiple directions, but for this measurement only the direction of the energy returning to the sensor within certain wavelengths is considered. Radiance is measured in watts per meter squared per steradian ($W\ m^{-2}\ sr^{-1}$) (Jensen, 2005).

Many of today's collection platforms provide relative brightness in the form of digital numbers (DNs). Due to the nature of DN, they are not equivalent across sensors. While this is sufficient for the analyst to complete visual comparisons, it does not allow brightness values to be compared between scenes, or over time. If a dataset is in DN, in order for a comparison to be completed one must first convert the data to radiance. The collection instrument's calibration data are required for this conversion. Although sensors on airborne platforms can be periodically calibrated, satellite systems are difficult to calibrate satellite systems

to absolute radiance once on orbit. One thing that can be done is known as a vicarious calibration, this process uses natural uniform surfaces (such as white sands or the moon) or calibrated targets to periodically check the calibration of their respective sensors (Campbell, 2007).

4.   Resolution

Resolution can be thought of as the ability a system has to record and display fine spatial, spectral, and radiometric detail (Campbell, 2007). Spectral resolution refers to the quantity and size of the examined wavelength intervals (bands) of the electromagnetic spectrum. Spatial resolution is a measurement of the smallest distance (either angular or linear) between two objects that can be determined by the sensor (Jensen, 2005). Often the instruments spectral sensitivity is specified using what is known as full width, half maximum (FWHM), which is the point where the response of the instrument reaches half of its maximum value (Figure 13). Even though the instrument limits reach past full width, half maximum, the response is too weak to be reliable (Campbell, 2007).
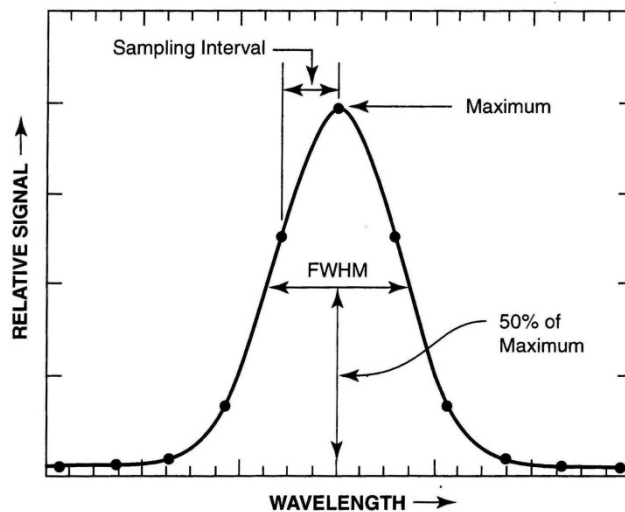
Figure 13.   Full Width, Half Maximum
The figure above shows full width half maximum (From Campbell, 2007).

There is also what is known as a temporal resolution, which refers to the sample time or the amount of time between data collects (Jensen, 2005). The

general practice of remote sensing is that there will seldom be high spatial, spectral, and temporal resolutions; more often there are required tradeoffs between these resolutions due to technological limitations.

5.   Remote Sensing through Water

Remote sensing though water brings in a variety of new challenges and considerations. For instance when imaging into water, refraction must be considered. Refraction is the bending of light that takes place when light passes between two mediums of different densities. The speed of light differs between different density objects, the higher the density the slower light travels. Different density objects have an index of refraction, which is the optical density of a substance. Snell's law $(\sin\theta_2 = \frac{n_1 \sin\theta_1}{n_2})$, which uses the index of refraction of both of the mediums (n_1 and n_2) and the angle of incidence of one medium can be used to calculate the amount of refraction that will take place (Jensen, 2005).

The water depth plays an important role in spectral characteristics of the light penetrating the water. The furthest penetration into a water column of pure water happens between 400–500 nanometers (nm), which is from violet to light blue. In Figure 14 it is shown how in the ultraviolet (<400nm), yellow (580nm), and into the infrared wavelengths (740–2500nm), the absorption rates are the dominating factor. This same figure also shows that the lowest amount of scattering and absorption in water takes place between 460–480nm, which is in the blue wavelength (Jensen, 2007). Another aspect to think about is whether there is inorganic or organic material suspended in the water, as it changes the absorption and scattering effects of the water. Storms can also play a role, increasing the turbidity and limiting the penetration of light into the water.
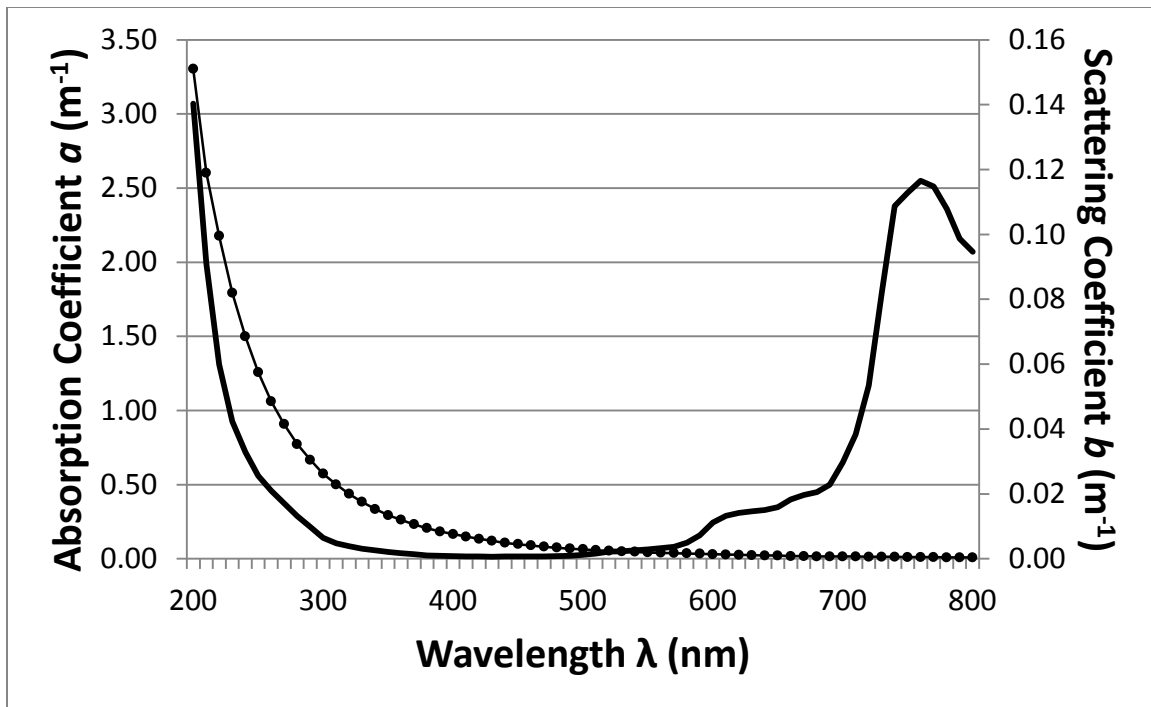
Figure 14.   Absorption and Scattering in Pure Sea Water
This graph shows the amount of absorption and scattering in pure sea water. The solid line is absorption and the dotted line is scattering coefficients (After Mobley, 1994).

When there are suspended materials within the water, it creates a challenge to extract useful information out of remote sensing data because it changes the spectra of the water. There is a large range of materials that can be suspended in bodies of water, varying in both source and size. Significant amounts of suspended sediment can be found in the near shore water, dramatically affecting the spectra seen by the sensor. The general rule of thumb is that water without suspended sediment will not appear as bright as water containing suspended sediment. This is not often a concern in remote sensing of deep ocean waters, as it is rare to find suspended sediment with a diameter greater than 1 μm in deep ocean water (Jensen, 2007).

Plankton and algae can also be found suspended in the water column. Plankton are tiny living organisms that are either animal, plants, or bacteria which have no means to resist being carried by the current. Depending if the plankton is

plant (phytoplankton), animal (zooplankton), or bacteria (bacterioplankton), it can contain or produce certain elements, which at high enough concentrations will play a role in the spectra of the water that is detected by a sensor. Some of the components in plankton can affect the spectra measured by sensors include carbon and chlorophyll. As an example, when phytoplankton levels rise, and consequently chlorophyll levels rise within the water column, the reflectance in the red and blue wavelength decreases, and the green reflectance increases (Jensen, 2007). Figure 15 illustrates spectral absorption of chlorophyll concentration across varying wavelengths (Mobley, 1994).
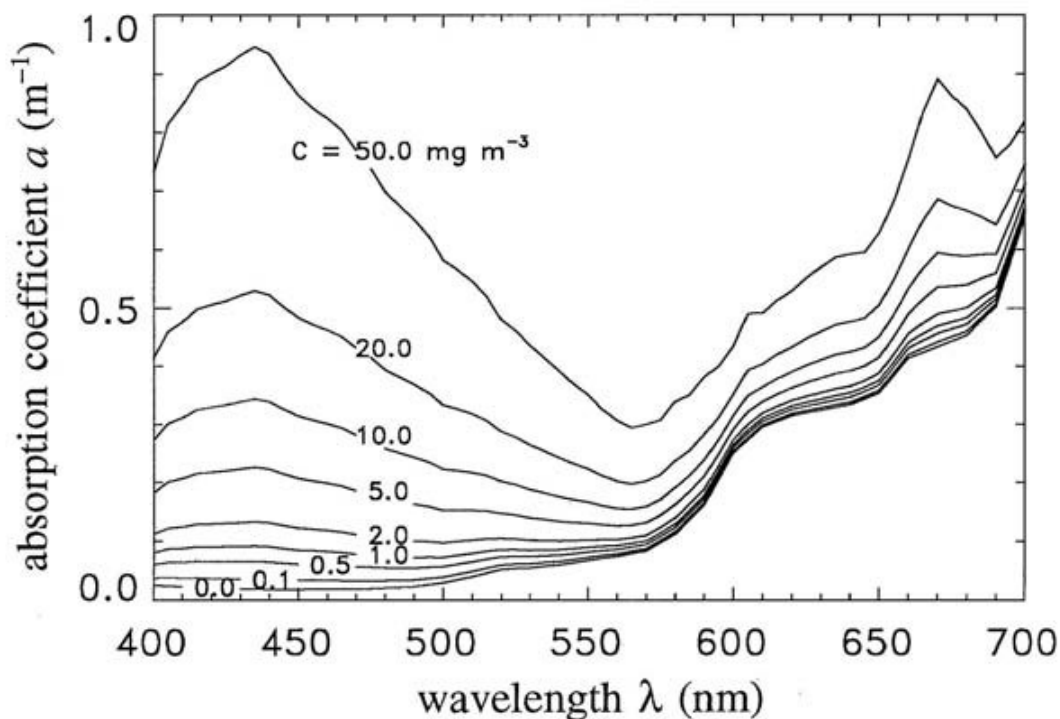
Figure 15.   Chlorophyll Concentrations
This graph shows a representation of the spectral absorption coefficient across wavelengths for a variety of chlorophyll concentrations (From Mobely, 1994)

When phytoplankton decompose it results in carbon dioxide, inorganic nitrogen, sulfur, and phosphorus, thus further playing a role in what is detected by the sensor. Bacterioplankton decomposes the organic matter created by the

zooplankton resulting in dissolved organic matter that can decrease the possible penetration of light into the water column. In coastal waters where there is so much inorganic material and dissolved organic matter that it is often hard to differentiate the effects of the phytoplankton (Jensen, 2007). With the large variety of debris found suspended in water, one can expect just as many possibilities of spectra measured. Figure 16 is an example of reflectance difference between pure water and water containing algae, which is dependent on wavelength.
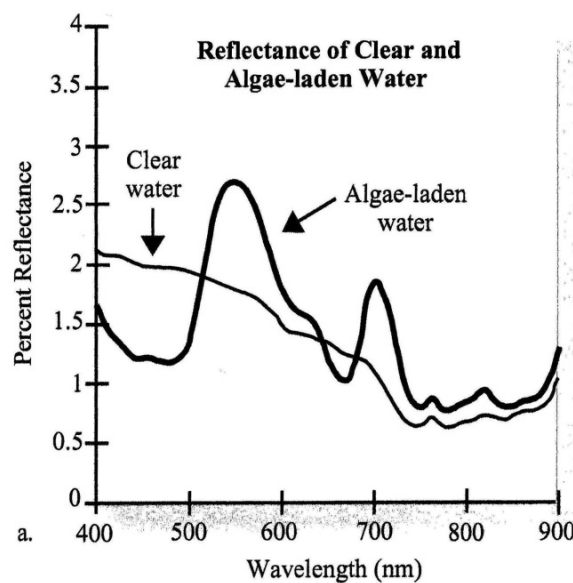
Figure 16.   Comparing Reflectance of Pure Water and Water Containing Algae
This figure shows how reflectance can differ depending if the water is clear or contains algae. The amount of variation depends on the wavelength
(From Jensen, 2007).

G.   MULTISPECTRAL IMAGING

The focus of this paper will be multispectral technology, in particular WorldView-2. Multispectral remote sensing is defined by Jensen (2005) as "the collection of reflected, emitted, or back-scattered energy from an object or area of interest in multiple bands (regions) of the electromagnetic spectrum" (p.44). Multispectral imagery provides spectral information about the surveyed area that

cannot be provided from a single spectral band. The advantage of multispectral over a traditional photograph is that a spectral profile is collected. This means for any given pixel in a data stack a profile can be created, with one axis representing the band collected and the other representing the brightness. Even though it may be thought that a large number of bands are required to identify a material by its spectrum, this is not always the case. Sometimes with a few bands placed in optimum positions, the required information can be determined. In multispectral imagery, data is obtained for a number of bands and is recorded as a cube of data containing spatial and spectral information (Jensen, 2005).

A DN, representing the brightness is associated with each pixel. The DN are organized as a matrix with each value related with a particular row and column. The data is in the form of a cube because each of the bands collected involves one of these matrices, and they are all registered to one another (Figure 17).
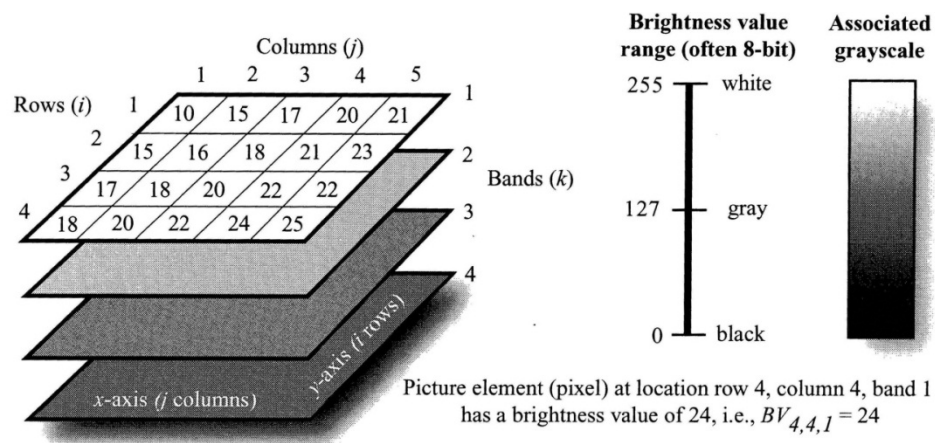
Figure 17.   Digital Imagery Stack
The above image is from Jensen (2005) and represents how data containing brightness values are stacked.

Multispectral data can be collected on either aircraft or spacecraft platforms. The platform used will play a role in how the data is returned to the analysts. If an aircraft is used it is not difficult for the data to just be returned after

flight, but in some cases, it is also possible for data to be transmitted to a ground station during flight. When a spacecraft is the collecting platform, the data must be directly transmitted to ground stations or relayed though other satellites and then transmitted to the ground. The percentage of electromagnetic radiation that hits the object and is reflected back is what the multispectral sensors measure. There are a number of different types of sensors that are used to collect multispectral images. These include traditional cameras with film, scanning mirrors, "pushbroom" linear arrays, "whiskbroom" linear arrays, and digital frame cameras that use area arrays; all of these can be seen is Figure 18 (Jensen, 2005).

Remote Sensing Systems Used to Collect Multispectral and Hyperspectral Imagery
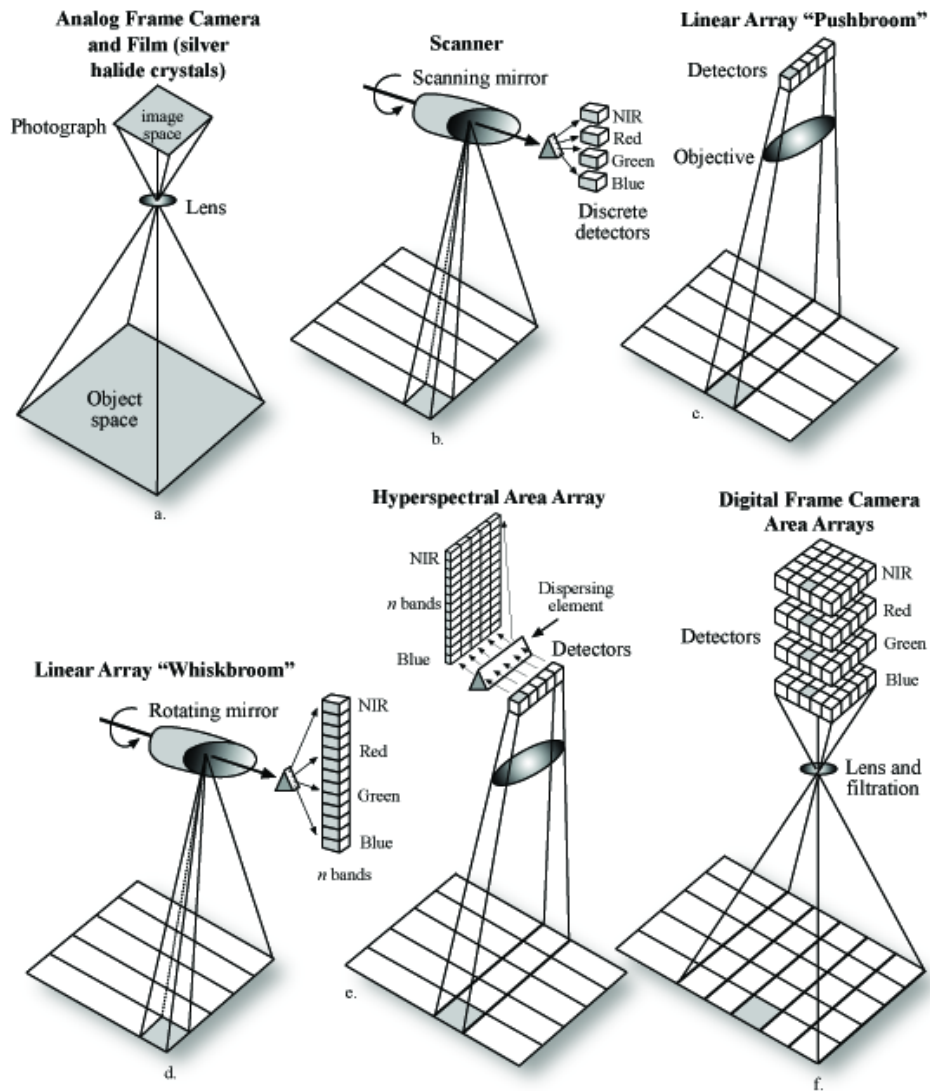
Figure 18.   Types of Sensors Used in Multispectral Remote Sensing. This image, from Jensen (2005), shows the different techniques used for collecting data. a) represents a traditional photographing technique, b) represents a multispectral technique that uses a scanning mirror and discrete detectors, c) uses linear arrays in a "pushbroom" technique, meaning that it pushes forward collecting one row after another, d) scanning mirror and linear array in a "whiskbroom" pattern that collects from side to side across one row at a time, e) linear and area arrays are used to collect data (note that e is a hyperspectral technique and does not pertain to this paper), f) digital frame camera that uses an area array technique.

1.   Atmospheric Correction

Due to the effects of the atmosphere, it is sometimes necessary to compensate for the effect of the atmosphere on data, to account for potential errors caused by scattering and absorption. In order to complete atmospheric correction other data must be available. It is required to know the atmospheric information for the time the data was collected, since atmospheric conditions are not always the same and there are many factors that can affect it. Atmospheric correction is not required with every data set and it is important to determine if it is required for the application of your mission. In cases where subtle differences in reflectance are important, atmospheric correction can be critical. If the study requires signatures to be used across time or space it is required that each dataset be atmospherically corrected for the cross comparison (Jensen, 2005).

2.   Eliminating Glint and Clutter

Another issue that may need to be addressed before images can be analyzed for targets beneath the ocean is eliminating glint and clutter in the image. Glint is a result of solar radiation reflecting off of a rough water surface and can often impede a sensor from looking below the water's surface. Glint happens most often in imagery from clear days when the sea surface is not flat and is hit with specular reflection of solar radiation. It is particularly a problem when high spatial resolution data is collected of shallow waters (Hedley et al., 2005). Sun-glint hinders the ability to identify features both on the bottom and in the water column, which can confuse further processing methods such as classifications (Edwards, 2012). One way that de-glinting is accomplished is by using spectral information from the near-infrared band to remove the sun-glint portion within the visible portion of the signal (Hedley et al., 2005). This method is only be appropriate for platforms that have both near-infrared and visible sensors. Another method for differentiating between the scattered and reflected light, is to utilize the fact that the light reflected from the surface will have a larger red component when it returns to the sensor (Silva & Abileah, 1998). Color

36

subtraction is yet another method, in which sea surface induced variance is removed using the understanding that blue and green light will have different water absorption effects (Barnes, Gilbert, Schoonmaker, & Rohr, 1999). Research continues to create algorithms which can remove effects of glint from the image.

De-cluttering can become important in naval mine detection. Traditional methods of mine detection classify mine-like materials, but can often have many false alarms, that are actually natural "clutter", such as coral reefs or rocky areas. Often the amount of clutter is greater than the actual targets, especially in extremely cluttered locations like reefs or rocky areas, leading to a higher rate of false alarms. After a mine-like object is detected, it is further investigated and identified. A high rate of false alarms can become an extreme waste of resources. Continuing research is needed in order to come up with a reliable automated method of identifying man-made objects.

3.   Principal Component Analysis

Principal component analysis is a common technique used with both multispectral imagery (MSI) and hyperspectral (HSI) data. This process transforms the original correlated spectral bands into a smaller set of uncorrelated variables that are easier to interpret. This newly transformed data structure can represent most of the information from the original data set. Principal component analysis rotates the axes of the original dataset, redistributing the brightness values into the new bands. The first new band is known as the first principal component (PC_1), the second principal component (PC_2) is orthogonal to PC_1 (uncorrelated). PC_1 is associated with the maximum amount of variance, and generally represents the average scene brightness. Higher order PC bands statistically show how the original bands may differ spectrally in the scene response.

In low dimensional (MSI) data, scatterplots of the PC_1/PC_2 values can be created representing most of the scene information. The correlation and quality

of those bands can be evaluated based on the variance or spread of the data. The original axes data are transformed to the principal component axes by applying transformation coefficients in a linear fashion to the original pixel values. The covariance matrix of the original dataset is used to complete the linear transformation. When a covariance matrix is used for the analysis, the result is a non-standardized principal components analysis. The process can also be completed using a correlation matrix, where the result is a standardized principal component analysis. In standardized principal component analysis, each band is given equal weight in creating the new component images. The resulting eigenvalues are often referred to as components. Within the matrix the non-diagonal eigenvalues can be ignored as they will all be equal to zero. In a square covariance matrix, the number of nonzero eigenvalues will be equal to the number of bands that were examined. The PC_1 will account for most of variance from the dataset and the variance will decrease with each consecutive component after that. Using the component and the original brightness values in the following formula, it is possible to calculate the new brightness value for the component (Jensen, 2005). Where n=the number of bands, a_{kp} = eigenvectors, and $BV_{i,j,k}$ = the brightness value for band k in row i, column j.

$$newBV_{i,\,j,\,p} = \sum_{k=1}^{n} a_{kp} BV_{i,\,j,\,k}$$

(1)

Completing this calculation for each of the dataset's pixels will result in the principal component 1 image dataset. Color composites can be created using principal components as the blue, green, and red bands. Often these composite are better at revealing subtle differences in color shading and distribution than traditional composites. Due to the fact that most of the variance of the dataset is found in the first few components it is possible in some instances to run analyses on these resulting principal component images, greatly reducing the amount of data to be processed (Jensen, 2005).

4.   Anomaly Detection

An anomaly in remote sensing is considered to be an area that is different, or irregular, from the rest of the image. In multispectral imagery, anomaly detection is done to locate pixels that have unusual spectral signatures or unusual spatial textures. Defining what qualifies as an interesting anomaly can be a difficult task for an analyst. For instance, the brightest pixels could be unlike most of the other pixels and therefore meets the definition of an anomaly, but that doesn't mean they are of interest. For this reason, it is not possible for analyst to say that one kind of feature will always be classified as an anomaly of interest (Theiler & Cai, 2003). It is known that multispectral imagery can be utilized to increase the detectability of targets with poor spatial distribution. It has also been shown that detection of objects can improve using multiple spectral bands when targets have a known spectral shape, even when the spectral characteristics are not known (Ashton & Schaum, 1998).

When searching for targets over a large area, low spatial resolution can be used to locate anomalies based on known background characteristics. While identification may not be possible using this technique, that could cue another sensor could further identify the mine. Another method that has proven effective for anomaly detection in multispectral imagery is spectral decorrelation filtering; however, this requires that you have a single type of terrain (single spectral signature) in your image (Ashton, 1998).

5.   Mixed Pixels

When trying to determine the spectrum of a target, the size of the target relative to the spatial resolution of the image (number of pixels per target) can play a large role. If the object is larger than the size of your pixels, then you can get a pure spectrum of the target. In this context a pure pixel is entirely made up of one material. If the target is smaller than the pixel size, then you will have what is known as a mixed pixel. A mixed pixel just means that there is not a single homogeneous material in the pixel. As a result there will be a brightness value

that is averaged and not a pure spectrum (also known as a signature) that can be used to identify an object. When a pixel contains the spectral responses from multiple features it is referred to as a composite signature (Campbell, 2007). The larger the pixels the higher probability of mixed pixels. It is critical for analysts to understand this and be aware of small aspects within the image that could result in mixed pixels.

H.   WORLDVIEW-2

Figure 19.   WorldView-2 (From Digital Globe, 2009a)

WorldView-2 is a high spectral resolution multispectral satellite that was launched in October 2009; and was the first commercial imagery satellite to gather eight bands (Padwick, Deskevich, Pacifici, & Smallwood, 2010). The satellite is in a sun-synchronous 100-minute orbit around the earth, at an altitude of 770 km (Digital Globe, 2012). The sensor is a pushbroom style imager, collecting one row of an image at a time using linear detector arrays (Updike & Comp, 2010). WorldView-2 has the ability to image 785,000 km^2 a day and averages a revisit time of 1.1 days (Digital Globe, 2012). The short revisit time makes WorldView-2 a valuable asset for monitoring a range of projects around the world. WorldView-2 is agile and has rapid retargeting capabilities, allowing for large single pass collection. This eliminates the problem of changing parameters

that are difficult to calibrate when smaller areas are collected and combined together. The spectral bands of WorldView-2 have a spatial resolution of 1.84m (depending on the angle of collection) covering the spectral range from 400nm-1050nm, and a panchromatic band that stretches from 450nm-800nm with a spatial resolution of 0.46m (Padwick et al., 2010; Digital Globe, 2009a). The high resolution allows this system to detect spectral differences in relatively small ground features. When designing WorldView-2 the traditional design was modified and four new color bands were added to the system, including: Coastal Blue (400–450nm), Yellow (585–625nm), Red Edge (705–745nm) and Near Infrared 2 (860–1040nm) (Digital Globe, 2009b).
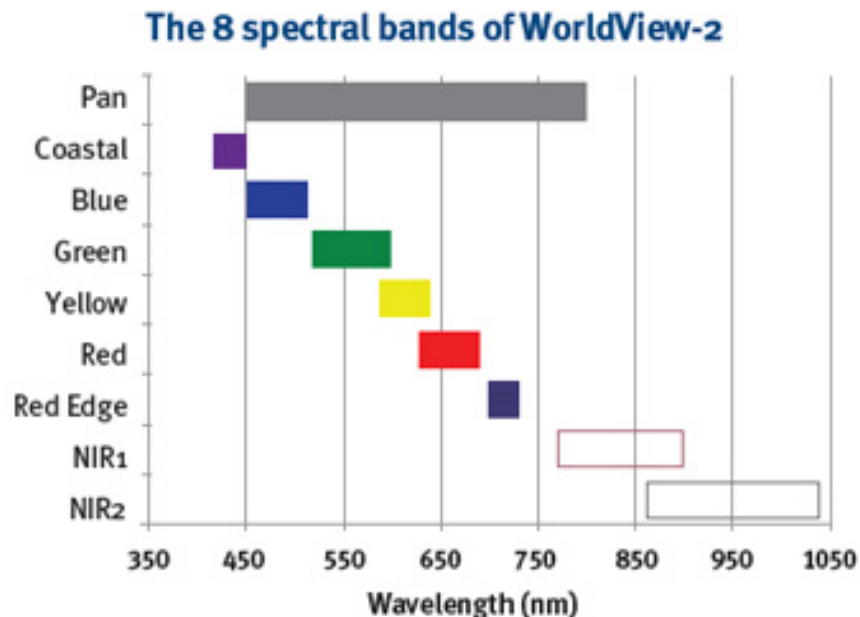
Figure 20.　　　Bands of WorldView-2
This figure show the range of the eight spectral bands of WorldView-2 (From Digital Globe, 2009b).

The focus of the WorldView-2 sensor was coastal and vegetation land cover types, mapping of benthic and wetland habitats, as well as water quality (Marchisio et al., 2010). This was the first satellite system to have a Coastal Blue detector (Digital Globe, 2009a). The intention of the Coastal Blue was to allow for vegetation identification analysis, bathymetric research that deals with chlorophyll

and water penetration, as well as atmospheric correction techniques (Digital Globe, 2009b). The Coastal Blue was included on the satellite to allow analysts the ability to calculate the ocean depths up to 20–30m (Digital Globe, 2009a). The other three bands were included to help with different aspects of vegetation studies (Digital Globe, 2009b). Due to the sharper channels and the continuous broad coverage, the satellite provides the possibility for better discrimination of spectral signatures than previous satellites (Marchisio, Pacifici, & Padwick 2010).

I.   MINE DETECTION

Utilizing imagery from multispectral and hyperspectral sensors has allowed the ISR community to detect and classify targets over a large area, while remaining at a distance (Leonard et al., 2008). There has been previous research locating naval mines using remote sensing technologies, however further research is needed to fully exploit the capabilities of the technology already in use, such as the WorldView-2. This is a complicated issue, as any capability has to be able to detect a variety of spectral signatures and spatial features, since naval mine are not built with standardize parameters and are always evolving.

Once an image has had any required pre-processing (including checking senor's calibration and atmospheric correction) the next step would be to have a process to detect mines that would be scarcely represented in the scene. There have been papers that present mine-detecting algorithms, such as Elbakary & Alam (2008), utilizing constrained energy minimization method of mine detection. In this algorithm the constrained energy minimization is used as a classifier that uses no information about the clutter in the scene and only the mine information for the training and locating potential mines. Since the sea is a highly variable environment, detection of naval mines becomes an even more difficult task then detecting terrestrial targets. The fact that mines are highly variable in size, shape and orientation adds another challenge for locating naval mines. A bulk of the research has focused on detecting targets that have known spectral signature, which is unrealistic in many circumstances. There are several reasons that this

will often not be useful. First, a complete understanding of the exact material, paint, or camouflage being used is not likely in many instances. Secondly, the ever-changing weather conditions mean that the atmospheric interference varies, which can produce different measured spectral signatures. Lastly, when looking for small targets that are sub-pixel in size the spectrum of the target is mixed with that of the background (Ashton, 1998).

THIS PAGE INTENTIONALLY LEFT BLANK

III. METHODS

A. DATA COLLECTION

In March 2012 multispectral data were collected over a known barnacle study taking place off the coast of La Jolla, California. The barnacle study involved objects in the water that were less than a meter in size. From this point, these objects will be referred to as targets for this study. The targets were painted black, green, blue, and white as detailed in Figure 21. Targets were located on the surface and at one, two, and three meters of depth. Buoys were put in place as markers of the study site.

Figure 21.   Target Layout

Targets one though three were all painted green. These targets were all below the surface at varying depths as follows: target one was two meters, target two was at three meter, and target three was at one meter. Targets four through six were all on the sea surface and varied in color: target four was white, target five was green, and target six was black. The targets trailing the buoys were on the surface and painted black, blue and green. The dot seen in the image by target three was a zodiac and it was only in the 21 March data set.

WorldView-2 data were obtained of the La Jolla barnacle test location, for three different dates. The dates acquired were 10 March, 13 March, and 21 March 2012. The data from 10 March 2012 were dropped from this study as there was too much sea surface glint to be useful. The 21 March imagery were used for the multispectral portion of the study, and both 13 March and 21 March data were used for the panchromatic analysis. The multispectral data had a resolution of two meters and the panchromatic imagery resolution was a half meter.

The two dates that were used in this study were not identical in collection. The average angle in which the data were collected varied. For the 13 March imagery the average target azimuth angle was 17° and the average angle off nadir was 21°. For the 21 March data the average target azimuth angle was 103° and the average angle off nadir was 9°. Both of the images were collected at the same time of the day. The 13 March data were collected at 11:02 AM (1902 UTC) and the 21 March imagery was at 11:07 AM (1907 UTC). The data obtained were at different product levels when it came from DigitalGlobe. The DigitalGlobe product levels refer to the radiometric and geometric correction that has already been completed on the WorldView-2 images. The 13 March data was received in LV2A format and the 21 March imagery was received in LV1B format. No further radiometric or geometric correction was completed on this data once it was received from DigitalGlobe.

The sea surface conditions varied between the two days. This was examined using Scripps Institution of Oceanography data from the La Jolla buoy (The Coastal Data Information Program [TCDIP], 2012). This buoy gathers data 45 minutes after every hour. For this study the values were averaged between the 1045 and 1145 collects. The wind and swell conditions varied between the two dates as shown in Table 1.

	Wind speed (m/s)	Wind Direction (degree)	Swell Height (m)	Average Time Between Swells (seconds)	Fastest Time Between Swell (seconds)
13 March 2012	0.59	351.5°	0.775	9.445	11.155
21 March 2012	0.455	49.5°	0.82	6.315	10.455

Table 1.   Sea Surface Conditions

Shown in this table is the variation between the sea surface conditions of the two datasets (TCDIP, 2012).

B.   ANALYSIS

The shapefile representing the known locations of the targets were created by Burt (2012) using half meter and one meter resolution hyperspectral data. Based on the multiple data collections, Burt was able to conclude the locations of the targets on 21 March, 2012. These locations tended to be about 20 meters off from the latitude/longitudes that were provided of the targets, from the people running the barnacle test. Due to the nature of moored targets in the ocean it is realistic to expect that the targets locations differ slightly on the data from 13 March 2012.

1.   Multispectral Data

a.   *RX-UTD Anomaly Detector on Multispectral Data*

ENVI was the geospatial imagery processing and analysis program that was used for this research. The scene was chipped out to include only the area of the barnacle test, and this was used for the remainder of this study. Through exploration of the data it was determined much of the intensity return was in the infrared bands, for this reason these bands were used for the anomaly detector. An RX-UTD anomaly detection was run on the two infrared bands (bands seven and eight) of the 21 March data. The default options were used for this analysis.

b.   *Principal Component Analysis on Multispectral Data*

A forward PCA was run on the 21 March data as a proof of concept. This analysis was run as both covariance and correlation matrices, however only the covariance results were further used in this study. The default options were used for this analysis. All eight bands of the PCA were examined. A region of interest (ROI) was created using band one of the covariance PCA image. The targets, buoy, and the zodiac were all considered targets. N-Dimensional (ND) visualizer was used for initial creation of the ROIs, which were used to separate out the targets from the background. This method could only separate the targets from the background with limited accuracy. N-D visualizer didn't separate out the targets from the background from the targets. Pixels that represented the zodiac were not segregated and found all over the visualization. For this reason, this process was followed by manually defining ROIs further by deleting and adding to the ROIs by individual pixels. The ROIs included a one pixel (2m) buffer around the targets to account for a subpixel target showing up as multiple pixels. This could be a result of possible effects from light scattering or refracting in the water vapor, as well as the fact that a point target in a scene will rarely appear as a point on the sensor; there can be some bleed over into other pixels. This could also account for the target location appearing a couple of meters off. There were 219 pixels in the resulting target ROI. A scatter plot was also created to compare band one and band two of the covariance PCA image.

c.   *Receiver Operating Characteristic Curves*

The next aspect of the study was to gather the data required to create a receiver operating characteristic (ROC) curve for the PCA image. This was done using band threshold to ROI tool, with all its default settings. ROIs were created for a variety of minimum values ranging from zero to -500, to include all the target pixel's values. The values for the minimum threshold levels were arbitrarily determined. These band threshold to ROIs were then compared to the target ROI to determine how many of the pixels in the target ROI were

detected. A pixel map was created to help in the process of detecting the number of target pixels in the threshold ROIs (Figure 22). For basic understanding the false positives and true positives were graphed against the threshold value used. Using this data a graph was created comparing the false positive rate to the true positive rate.
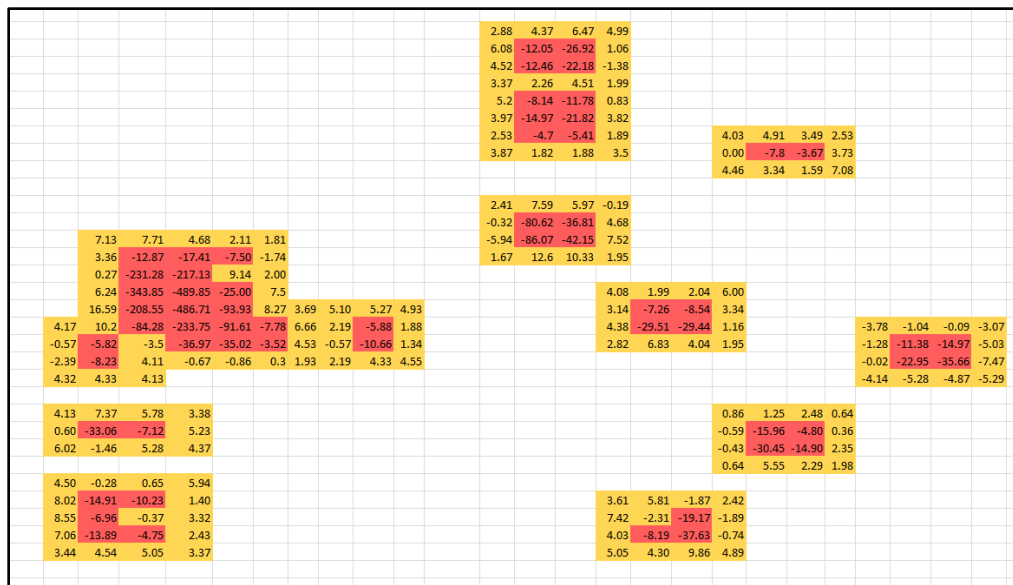

Figure 22.   Pixel Map of PC Band 1 Results

This pixel map was used to identify and count the number of target pixels detected in the threshold process. The map is not to scale but rather a basic representation of the targets seen in band 1 from the PCA. The cells highlighted in red represent the pixels that were determined to be targets based on inspection of the 21 March multispectral scene. The orange highlighted cells are the one pixel buffer that was placed around the known target. All of the highlighted cells were collectively considered target pixels. The values within the cells are the digital number of the pixel to which they correspond.

The data for a ROC curve of the RX-UTD analysis was also collected. The ROI of the targets from the PCA was brought into the RX-UTD image, in order to determine which of the pixels appeared as targets in the RX-UTD results were true targets. There were 80 pixels in the RX-UTD image that were targets. The resulting pixels were then used as the targets and Band Threshold to ROI tool was once again utilized with all the default settings. The minimum band threshold values for this analysis ranged from zero to 500, in

order to cover the DN of the RX-UTD target pixels. Another pixel map was created of this image and was used in determining the counts for the ROC curves.
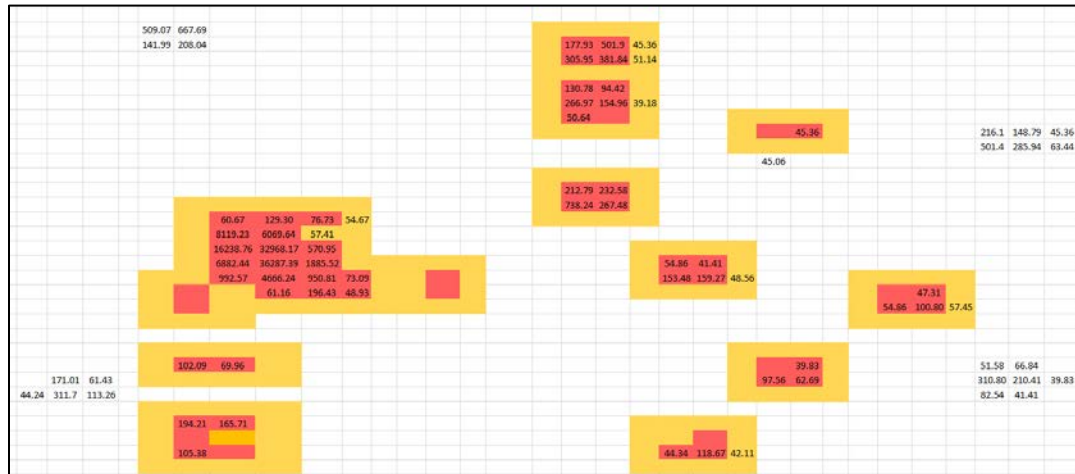

Figure 23.   Pixel Map of RX-UTD Analysis Results

This map was the pixel map that was used to show the detections of targets in the RX-UTD results. This map is not to scale but is a basic representation of the pixels in the image being examined. The colored cells were brought over from the PCA. These were being used as " ground truth" to help determine where the targets should appear in the RX-UTD analysis. The cells containing numbers represent the pixels that appeared as targets in the RX-UTD analysis. The number that are not highlighted are areas where the RX-UTD came up with a false positive. The numbers in the cells are the digital numbers of that pixel.

ROC curves were then calculated for both the PCA image as well as the RX-UTD image. The total pixels of the image were obtained from ENVI, and totaled 728,340 for both of the images. The true positive was the number of pixels that were targets and appeared as targets in the image. True negative is described as a pixel that was not a target, and no target was detected in the analysis. A false positive represents a pixel that the analysis calls a target but is not truly a target. False negative is the term used for pixels that did not detect a target where no target existed. The true positive rate was calculated by the true positive divided by the true positive plus the false negative. Similarly, the false positive rate is calculated by dividing the false positive by the false positive plus the true negative.

2. Panchromatic Data Analysis

The panchromatic data for 13 March and 21 March of the same location were also examined for this research. Once again the data was chipped to only include the barnacle study location for this work. This data was visually examined to locate targets. Digital numbers were collected from the numbered targets that were visible in the image. Statistics were gathered on the data chip, which included: minimum, maximum, mean, standard deviation. For both the dates the default stretches in the enhance menu were examined to determine if the targets could be highlighted.

To improve upon the image of the targets the histogram stretch tool was used. The bars within the histogram stretch tool, which limits the values displayed, were moved until the noise was mostly eliminated from an image of possible targets. The optimum location of these bars were determined by visual inspection. Smoothing was applied to the image after the stretch to determine if that would improve pulling out the targets from the background.

Filters were also used to try to automate the improvement of images of possible targets. All of the convolutions and morphology filters found in ENVI were applied on these data sets. The convolution filters included low pass, high pass, Laplacian, directional, Gaussian high pass, Gaussian low pass, median, Sobel and Roberts. The morphology filters that were tested were: erode, dilate, opening, and closing. Adaptive filters were also used, including: Lee, enhanced filter, frost, enhanced frost, gamma, Kuan, local sigma, and bit error. The final two filters that were used on the data were the texture and forward FFT. For further understanding the statistics were run on the frost filter. Target five was used for this analysis, in particular pixel 9291, 11514. Linear stretches were applied to these images and the color of these results was then inverted for better display.

IV. OBSERVATIONS & ANALYSIS

A. MULTISPECTRAL DATA

1. RX-UTD Anomaly Detector on Multispectral Data

The results from the RX-UTD anomaly analysis of bands seven and eight were partially successful. The buoys and some of their trailing targets were reported as anomalies. The surface targets (four through six) were all detected. The zodiac appeared the brightest in these results. Target three could potentially be contributing to the intensity near the zodiac, however the zodiac is over powering this small portion of the image, and the target is not distinguishable from the zodiac.
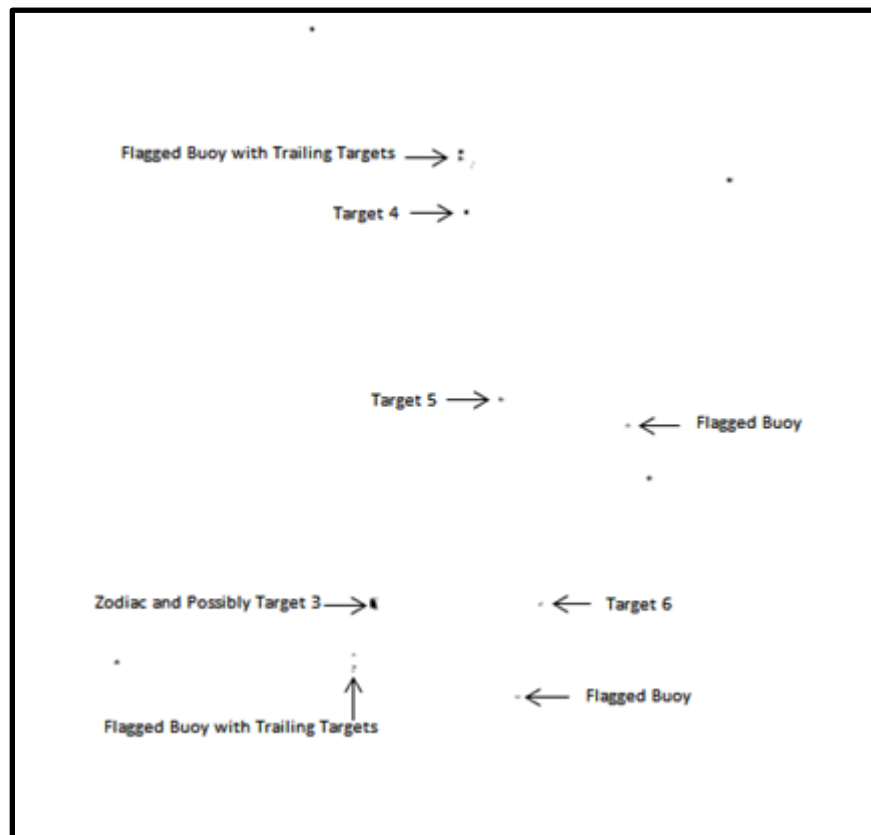

Figure 24.   RX-UTD Anomaly Detection Results
This image provides the results of the RX-UTD anomaly analysis. Colors were inverted from original results to better display targets.

2.   Principal Component Analysis on Multispectral Data

The covariance PCA of band one results provides an image that nicely represents the locations of the targets. Most of the targets appear in this analysis. Not all of the targets that are trailing behind the buoys are distinguished in this image. Potentially if the targets are floating close enough together they might be showing up as one target in the image, or not all of the targets are being revealed. The submerged targets are dimer but remain visible. As expected, the zodiac is the brightest target in the image. Target three remains distinguishable from the zodiac in this method, unlike in the RX-UTD analysis. The other seven bands were examined, and didn't represent the data as well as band one. The higher the band the more noise it contained. This covariance PCA result was the one considered further in this study.

The scatter plot comparing PC band 1 and band 2 separated out some of the targets from the background. The x-axis represents intensity, and the y-axis represents color. The densest area of pixels represents the background. The pixels surrounding it more closely are mostly targets, including the zodiac. The pixels furthest out from the background are pixels from the zodiac. These pixels have the highest intensity and the most color.
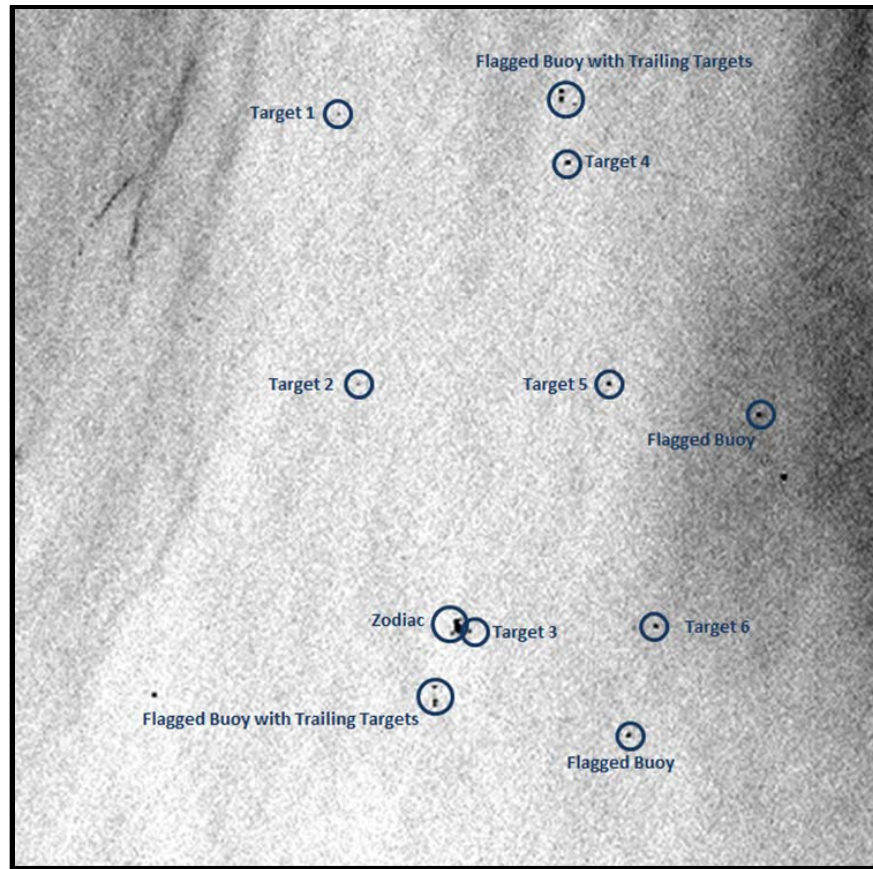
Figure 25.   Covariance Principal Component Analysis Result
This figure represents band one of the covariance principal component analysis.
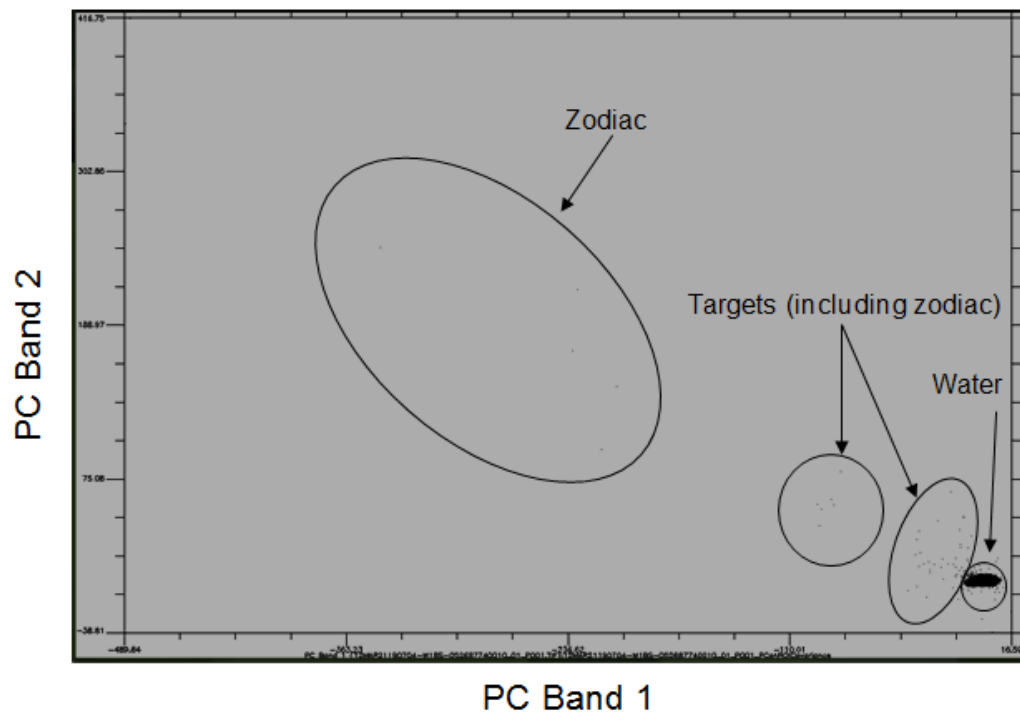
Figure 26.   Scatter Plot of PCA Band 1 and Band 2

The PCA was also run using the correlation matrix. Figure 27 illustrates the result of band one after this analysis. As in the covariance results, band one produced the best results and the higher bands contained greater levels of noise. Most of the targets are again revealed in this process, however not as clearly as the covariance matrix PCA results. There is still the issue with the targets trailing behind the buoy all being discernible as in the covariance analysis. The higher contrast in the results makes it a less clear representation of the target's location. Targets one and two, the two and three meter submerged targets, are becoming more difficult to determine. In the bright area on the right side of the image the flagged buoy is difficult to distinguish in this result. Target three is distinct from the zodiac.
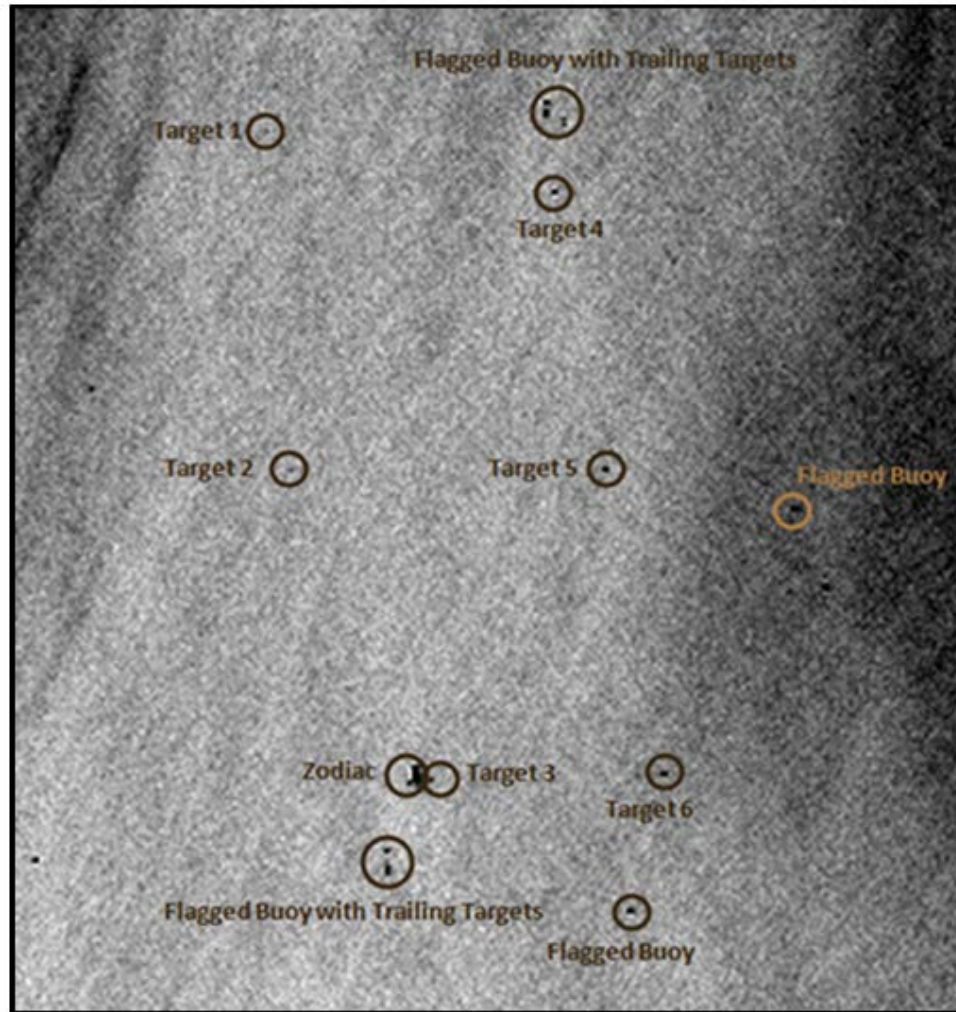
Figure 27.   Correlation Principal Component Analysis Result
This is band one results for the correlation principal component analysis. For improved display of the targets the colors of the image were inversed.

3.   Receiver Operating Characteristic Curves

The tables in this section display the numbers that were gathered and calculated for the ROC curves (Tables 2 and 3). The first step for basic understanding was to graph both the true positives and false positives against the threshold values for the PCA and RX-UTD analysis (Figure 28 and 29). In the results for the PCA it is found that no matter the threshold entered the result is a very large amount of false positives. The number of true positives were found to

increase as the threshold value got smaller. Examining the RX-UTD results it is found that the levels of false positives is not as extreme as the PCA results, but still contains quite a few. The overall pattern for both graphs is that as the threshold value decreases the amount of true and false positives increase.

The PCA ROC curve shows that the overall trend is when the rate of true positives increases so does the rate of false positives. The results of the ROC curves show that PCA is good method. The further the lift above the diagonal is in a ROC, the better the method. A ROC curve resulting in a diagonal line up from zero tells you the results are random. The RX-UTD results are closer to a diagonal line and then flattens out. Based on this, the PCA method is stronger than the RX-UTD method (Figure 30). Another aspect that must be considered is that a larger sample size could have helped improve the true picture of these methods.

Min DN Threshold	Total Pixel in Threshold	Total Target Pixels	True Positive	True Negative	False Positive	False Negative	TPR	FPR
0	103560	219	127	624688	103433	92	0.58	0.142054685965657
-5	138863	219	159	589417	138704	60	0.73	0.190495810449087
-10	157274	219	178	571025	157096	41	0.81	0.215755348355562
-15	157570	219	190	570741	157380	29	0.87	0.216145393416754
-20	157576	219	193	570738	157383	26	0.88	0.216149513611062
-25	157580	219	196	570737	157384	23	0.89	0.216150887009165
-30	157584	219	199	570736	157385	20	0.91	0.216152260407267
-35	157587	219	201	570735	157386	18	0.92	0.216153633805370
-40	157593	219	206	570734	157387	13	0.94	0.216155007203473
-60	157594	219	207	570734	157387	12	0.95	0.216155007203473
-80	157594	219	207	570734	157387	12	0.95	0.216155007203473
-100	157601	219	212	570732	157389	7	0.97	0.216157753999679
-150	157601	219	212	570732	157389	7	0.97	0.216157753999679
-200	157602	219	212	570731	157390	7	0.97	0.216159127397781
-250	157606	219	216	570731	157390	3	0.99	0.216159127397781
-300	157606	219	216	570731	157390	3	0.99	0.216159127397781
-350	157607	219	217	570731	157390	2	0.99	0.216159127397781
-400	157607	219	217	570731	157390	2	0.99	0.216159127397781
-450	157607	219	217	570731	157390	2	0.99	0.216159127397781
-500	157609	219	219	570731	157390	0	1.00	0.216159127397781

Table 2.   Numbers used for the PCA ROC Curve
The values in this table were those used to create the ROC curve for the PCA image.

Min DN Threshold	Total Pixel in Threshold	Total Target Pixels	True Positive	True Negative	False Positive	False Negative	TPR	FPR
500	16	80	13	728257	3	37	0.16	4.11941E-06
400	16	80	13	728257	3	67	0.16	4.11941E-06
300	20	80	15	728255	5	65	0.19	6.86568E-06
200	28	80	19	728251	9	61	0.24	1.23582E-05
175	31	80	22	728251	9	58	0.28	1.23582E-05
150	36	80	16	728250	10	54	0.33	1.37314E-05
125	40	80	28	728248	12	52	0.35	1.64776E-05
100	45	80	32	728247	13	48	0.40	1.78508E-05
90	47	80	34	728247	13	46	0.43	1.78508E-05
80	48	80	34	728246	14	46	0.45	1.92239E-05
70	50	80	36	428246	14	44	0.50	1.92239E-05
60	57	80	40	728243	17	40	0.58	2.33433E-05
50	65	80	46	728241	19	34	0.69	2.60896E-05
40	77	80	55	728238	22	25	0.71	3.02090E-05
30	89	80	57	728228	32	23	0.71	4.39404E-05
20	136	80	57	728181	79	23	0.71	1.000108478
15	686	80	57	727631	629	23	0.71	0.000863703
10	3562	80	57	724755	3505	23	0.71	0.004812842
5	18065	80	57	710252	18008	23	0.71	0.024727433
0	86078	80	57	642239	86021	23	0.71	0.118118529

Table 3.   Numbers for the RX-UTD ROC Curve

The images in this table were used to create the ROC curve for the RX-UTD image.
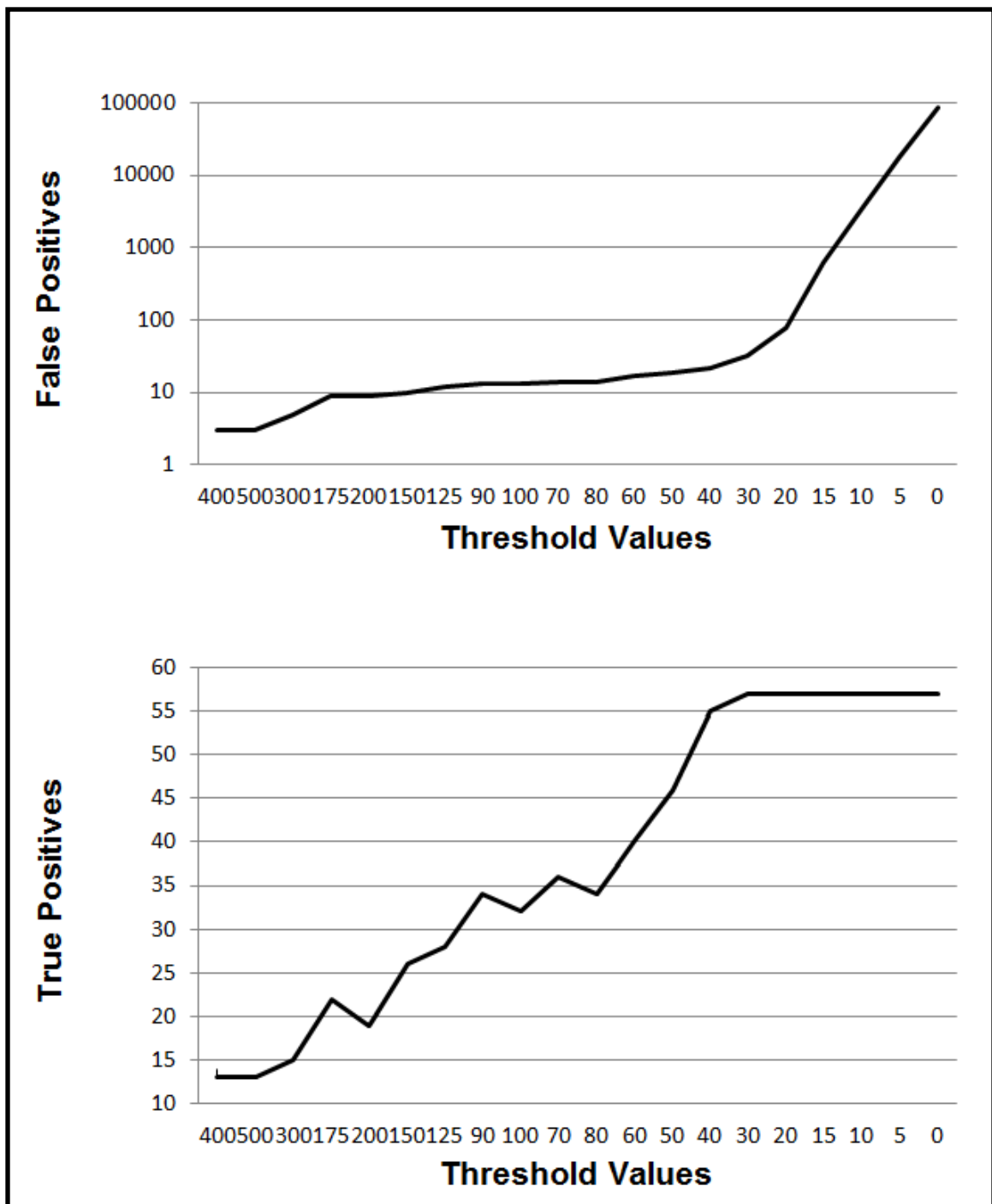
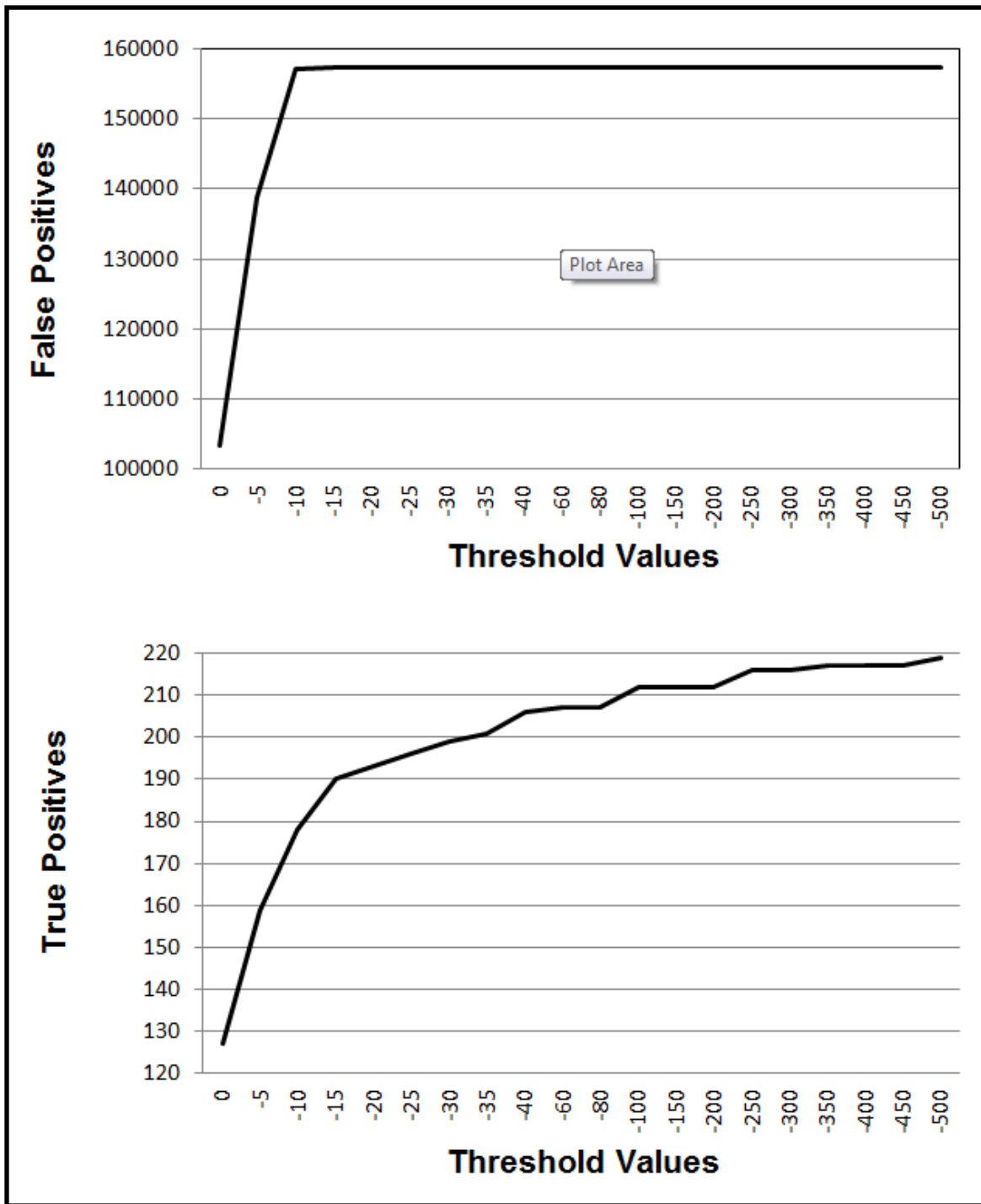Figure 28.   RX-UTD Thresholds
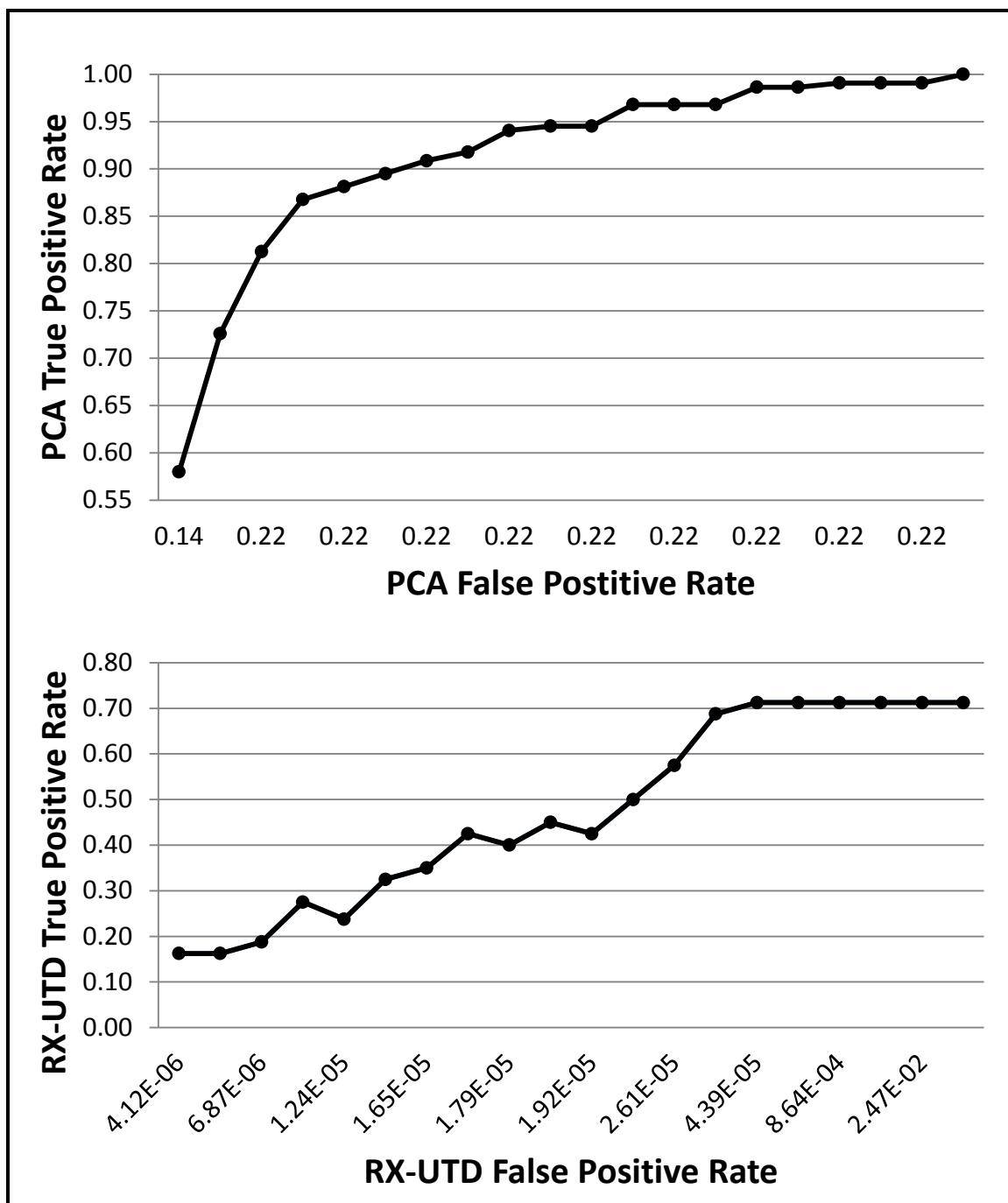
Figure 29.   PCA Band 1Thresholds

Figure 30. Resulting ROC Curves

The top graph is the resulting ROC curve for the PCA band one image. The lower graph is the ROC curve based off of the RX-UTD analysis. As seen in Table 2 and 3, differences between the false positive rates is extremely small.

B. PANCHROMATIC DATA ANALYSIS

With its high resolution, the panchromatic data allows us to visually observe a majority of the targets. The following figures illustrate what is visible in the panchromatic data. Since the high resolution covers a large area, smaller areas where targets are present are displayed. Tables four and seven indicate a digital number from the numbered targets that were visable in the image. Statistics and how many pixels are contained in each value range are given for each of the dates.

1. Visual Inspection

a. 13 March 2012

The panchromatic data from 13 March reveals a majority of the targets. They appear as brighter pixels in the image. The targets that remained unexposed in the panchromatic image were one and six as well as some of the targets trailing the buoys. The DN values for the numbered targets apparent in this image range from 130-362. The DN values of the chip have nearly the same range at 120-362 (Table 5). Looking at the range of the data it is found that 99.98% of the data is located between the DNs of 120 and 139 and 55.66% between DNs 120 and 129. The histogram of the data does not show a good separation between the targets and the background. There were two targets that appear together within the east flagged buoy and the south buoy that has trailing targets behind it. There were a few other points that contribute to the histogram as a single point for that value. The pixels making up the white target are an example of this. There were four pixels with DNs ranging between 239 and 362. As they were single pixels they did not become obvious in the histogram.
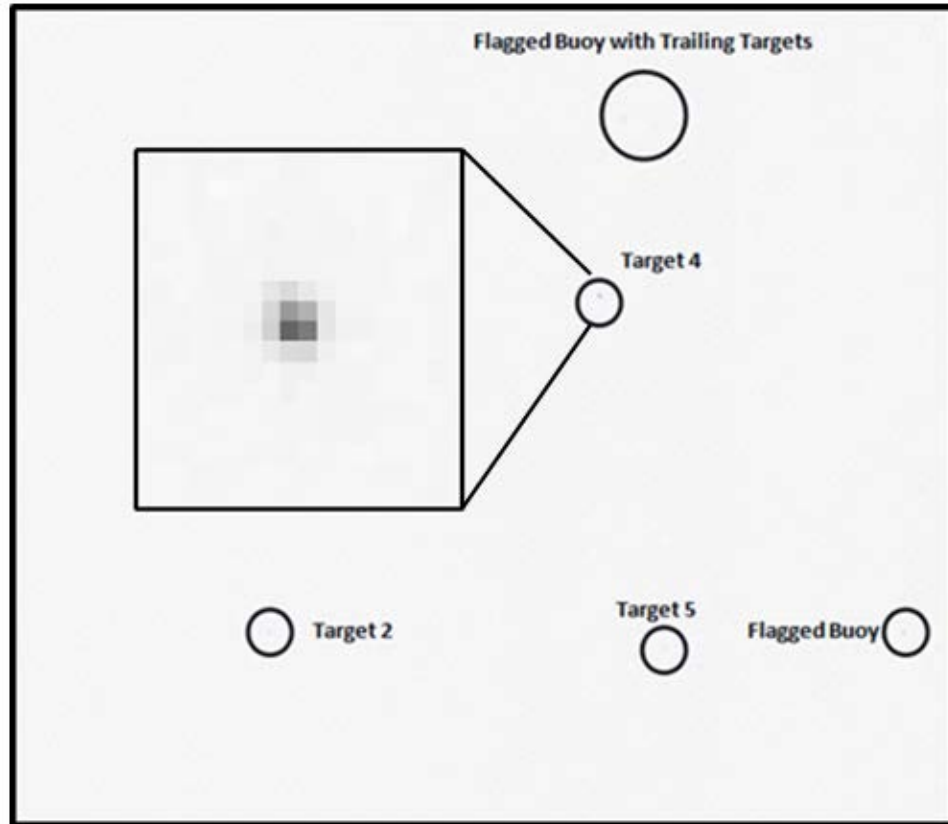
Figure 31.   Northern End of Survey Area from 13 March Data

Targets in northern portion of survey area were observed in visual inspection of the panchromatic data. While hard to depict in this image the targets were easier to depict in ENVI. Target four is enlarged to illistrate what is visable during analysis. In order to better represent the data the colors were inverted.
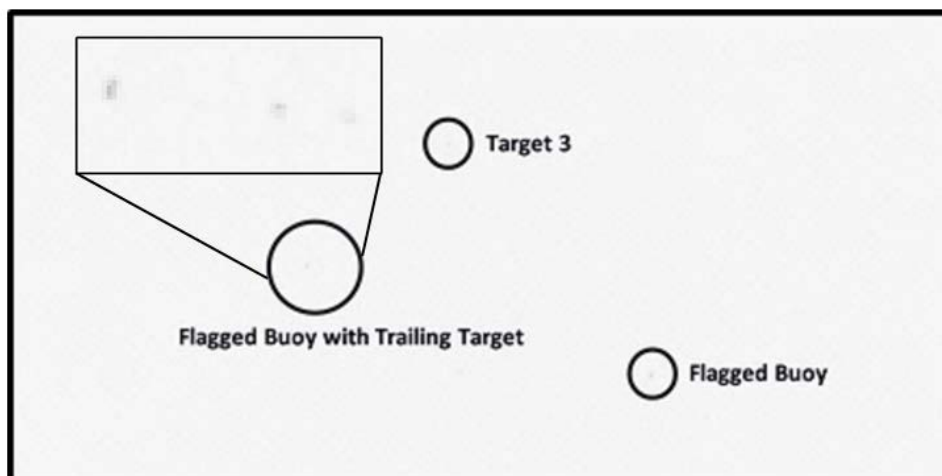
Figure 32.   Southern End of Survey Area from 13 March Data
Representation of southern end of study site targets found in visual inspection of panchromatic data is conveyed in this figure. To provide reader better visibility colors were inverted.

Target Number	DN	Color	Depth
Target 2	176	Green	3 m
Target 3	130	Green	1 m
Target 4	362	White	Surface
Target 5	155	Green	Surface
Average DN	215		

Table 4.   DN Values for Visible Targets in Panchromatic 13 March Data Chip

Min	120
Max	362
Mean	129.3
Standard deviation	1.87

Table 5.   Statistical Results for Panchromatic 13 March Data Chip

Value Range	Number of Points
300-362	2
250-299	1
200-249	5
150-199	151
140-149	664
130-139	1667439
125-129	2079034
120-124	15289

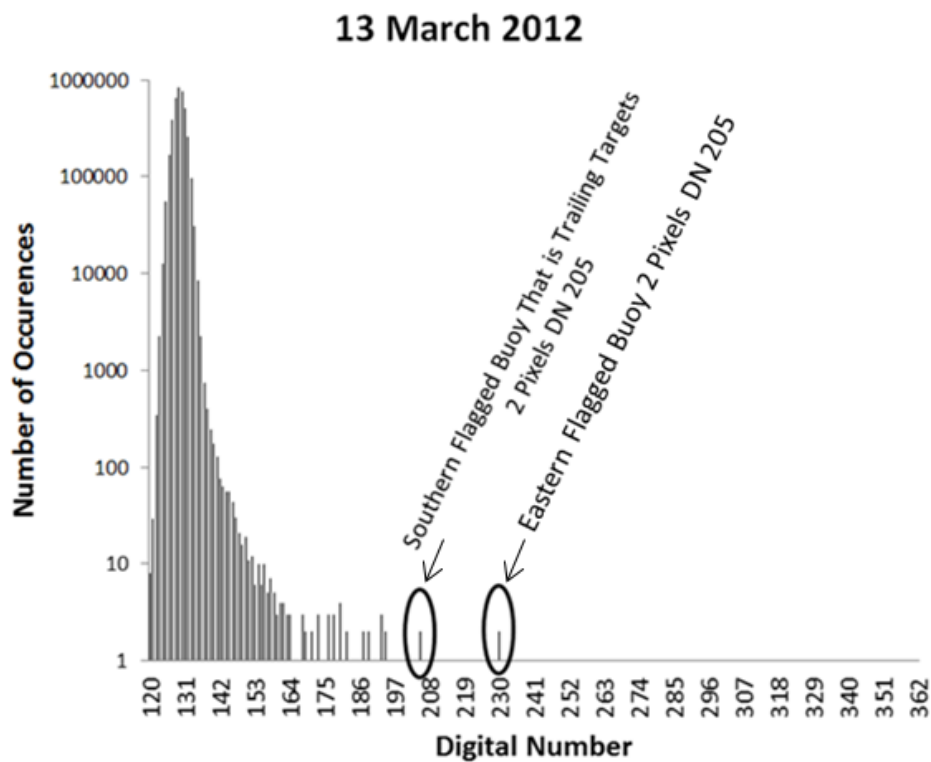Table 6.   Pixel Counts of Panchromatic 13 March Data Chip

Figure 33.   Histogram of Digital Numbers for Panchromatic 13 March Data

b.   21 March 2012

The 21 March panchromatic data was also rather successful at visually exposing the majority of the targets. The targets that were not apparent were targets one and two as well some of the trailing targets. While targets in the following images are hard to distinguish, they were easier to depict in ENVI. For

better visibility, the color of the image was inverted. The DNs for the apparent targets in this image chip have a greater range then the 13 March data. In this image the DN range from 80 to 1204. Like the other dataset a majority of the pixels of this image are found in a small range. For this dataset 99.99% of the data is found between the DNs of 80 and 100, and 96.09% of the data had DNs that range from 80-89. Like the 13 March data the resulting histogram from the 21 March data does not provide a clear cut result in separating out the background from a majority of the targets. The target that plays the main role in this histogram is the zodiac. The zodiac contains pixels with a wide variety of DNs that over power single pixels of any of the other targets.
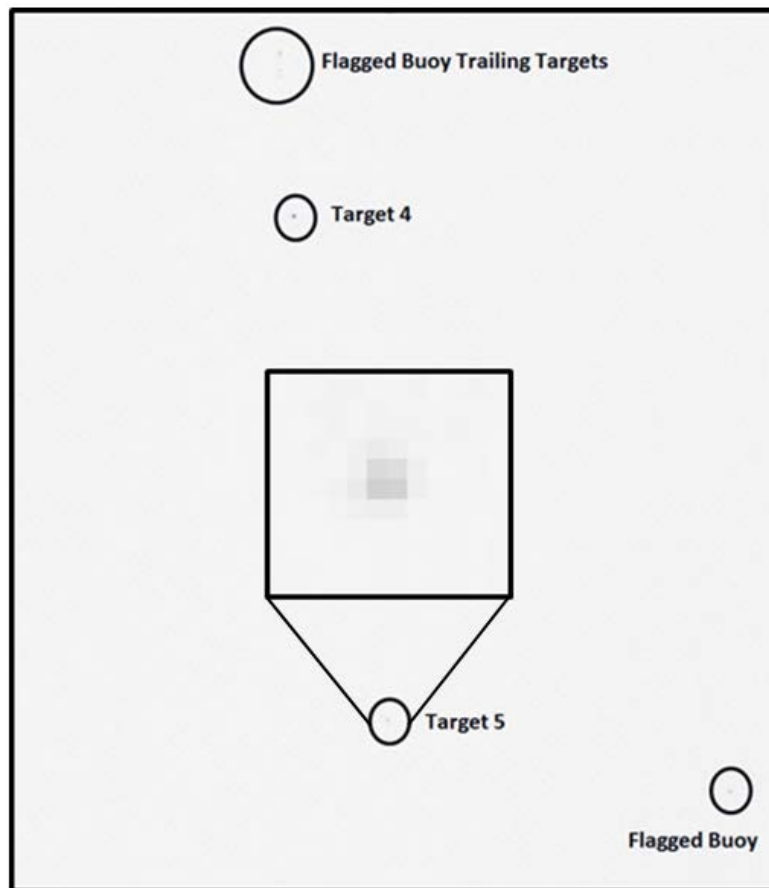

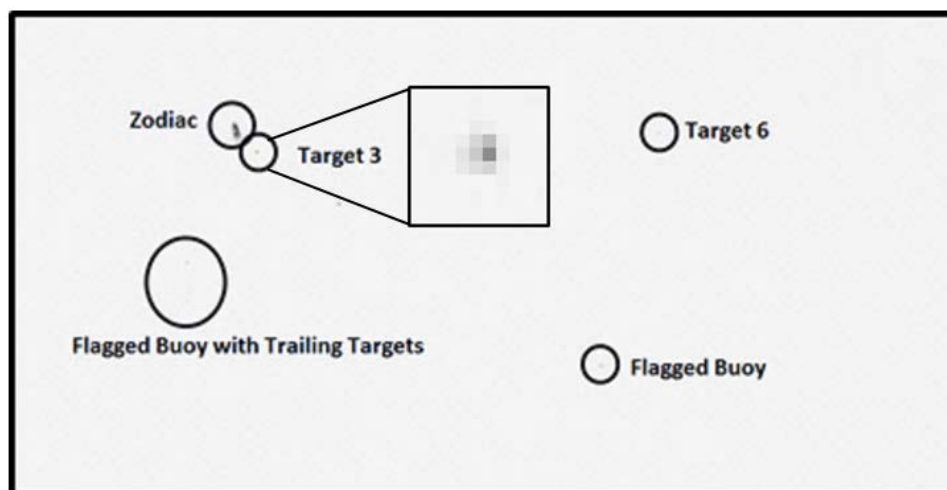Figure 34.　　Northern End of Survey Area from 21 March Data

Figure 35.   Southern End of Survey Area from 13 March Data

Target Number	DN	Color	Depth
Target 3	279	Green	1 m
Target 4	301	White	Surface
Target 5	152	Green	Surface
Target 6	130	Black	Surface
Average DN	**215**		

Table 7.   DN Values for Visible Targets in Panchromatic 21 March Data Chip

Min	80
Max	779
Mean	88.3
Stdev	1.91

Table 8.   Statistical results for Panchromatic 21 March Data Chip

Value Range	Number of Points
501-779	93
301-500	29
201-300	33
151-200	35
126-150	55
101-125	211
90-100	284821
80-89	7007614

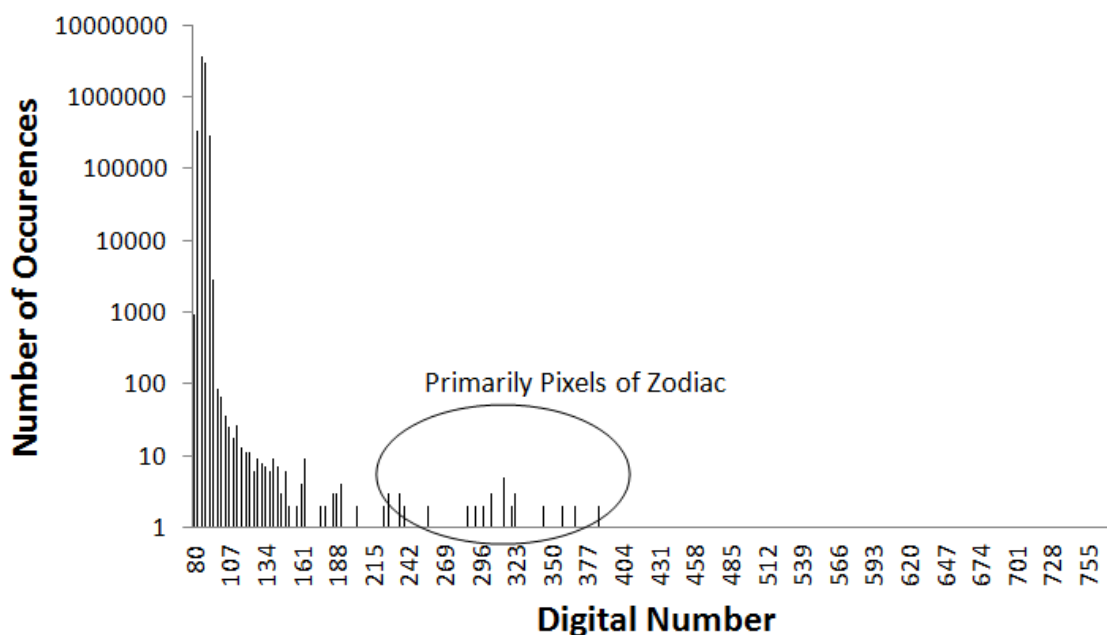Table 9.   Pixel Counts of the Panchromatic 21 March Data Chip

21 March 2012

Figure 36.　　　Histogram of Digital Numbers for Panchromatic 13 March Data

2.　　Default Stretches

For both panchromatic data sets, all of the ENVI default stretches discussed earlier were applied. Over all, the default stretches that appeared to be the most useful for this kind of work were the linear and the square root. These stretches were successful at separating out some of the targets from the background. None of the default stretches were effective at locating all of the targets. As in the above results, unfortunately the targets appear dim but were distinguishable in ENVI.

a.　　13 March 2012

Linear and image linear 0-255 were two default stretches that were the most successful on the 13 March 2012 data. Using the linear stretch and the image linear 0-255 stretch some of the targets were found in the scene. All of the buoys and some of the targets that were attached to two of the buoys were represented with these stretches. Targets two, four, and five were also depicted

with these stretches. Target three was potentially seen in Figure 35 however with the level of noise it is not possible to know for sure.
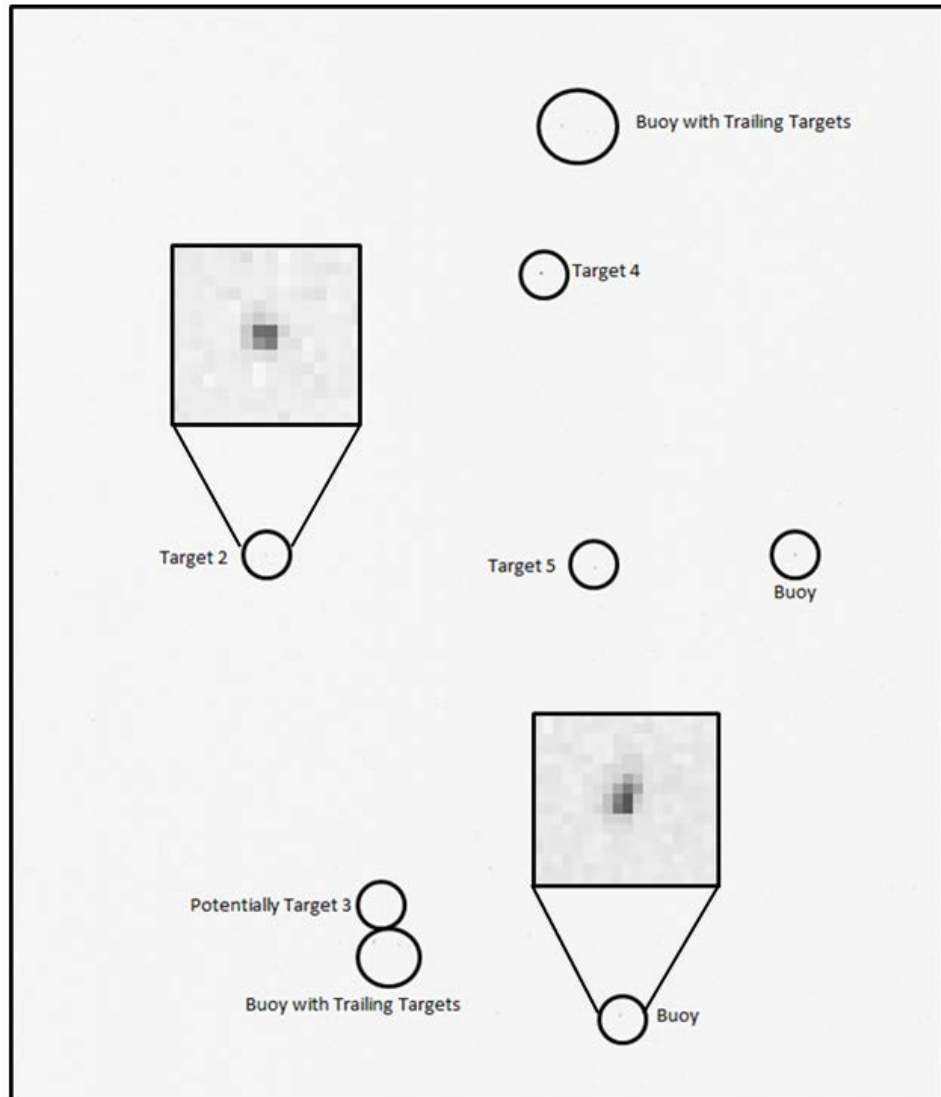

Figure 37.　　13 March Linear Stretch Results
Resulting image of the linear default stretch applied to the image. In order to improve the visualization the colors of the image were inverted.
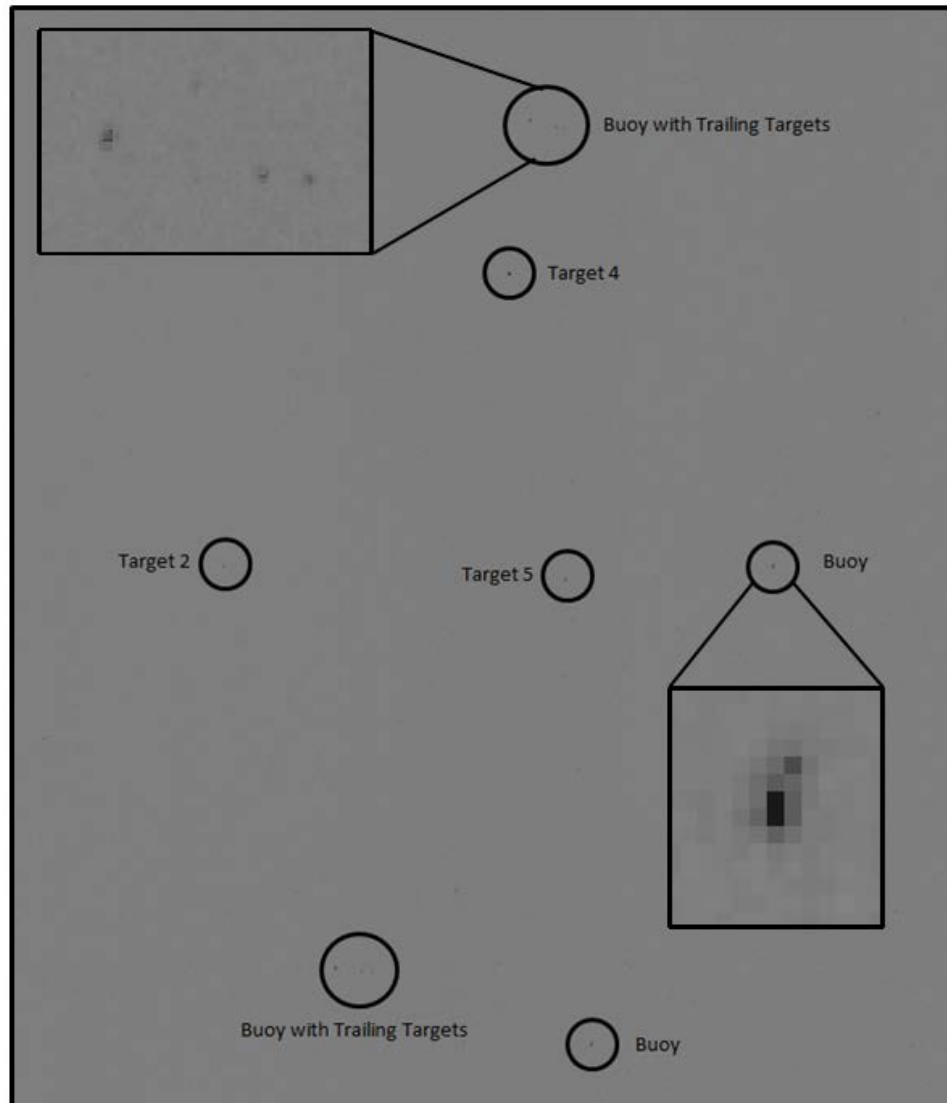
Figure 38.   13 March Linear 0-255 Stretch Results

For these results an linear 0-255 stretch was applied to the 13 March data. To provide better representation of the targets the image colors were inverted.

b.   21 March 2012

The two default stretches that worked best with the 21 March 2012 data set were scroll square root and image linear 0-255. Both of the stretches picked up most of the targets. In both of these stretches, targets three though six were evident. The zodiac was the most obvious aspect in the results of both of

these stretches. All of the buoys were visible, however all of the targets attached to the two buoys did not all become apparent with this method.
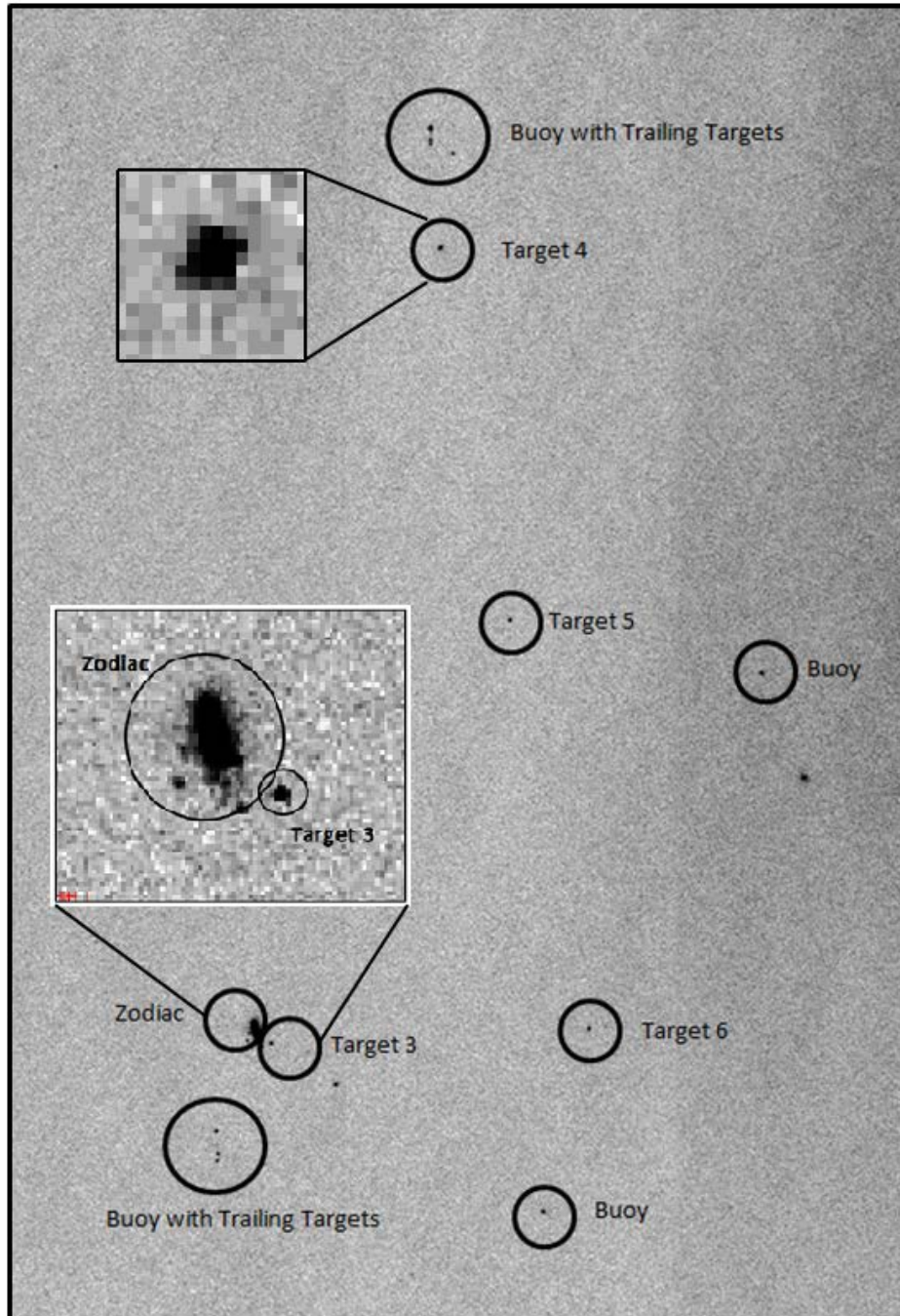

Figure 39.　　21 March Square Root Results
A default square root stretch was applied to the 21 March dataset, providing these results. For better presentation the colors were inverted.
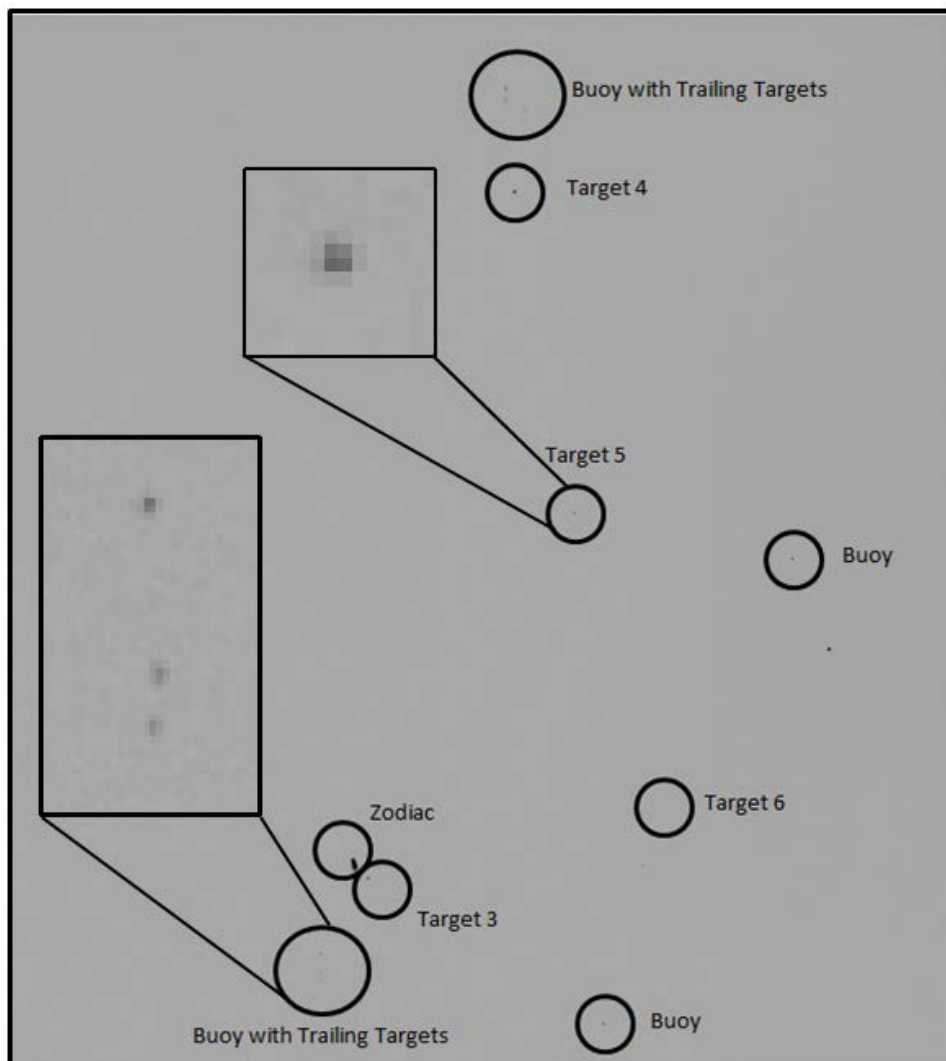
Figure 40.   21 March Enhance Linear 0-255 Results
This image is the result of an linear stretch 0-255 applied to the 21 March data. Following this the colors of the resulting image were inverted.

3.   Histogram Stretch

a.   *13 March 2012*

For the 13 March data set, the stretch was set from 138 to 196. Targets one, six, and some of the trailing buoys were not evident in this image. The submerged targets are the dimmest in this stretch. Smoothing was applied to this image, resulting in further elimination of targets. Targets, while hard to see in these image, they were easier to see in ENVI.
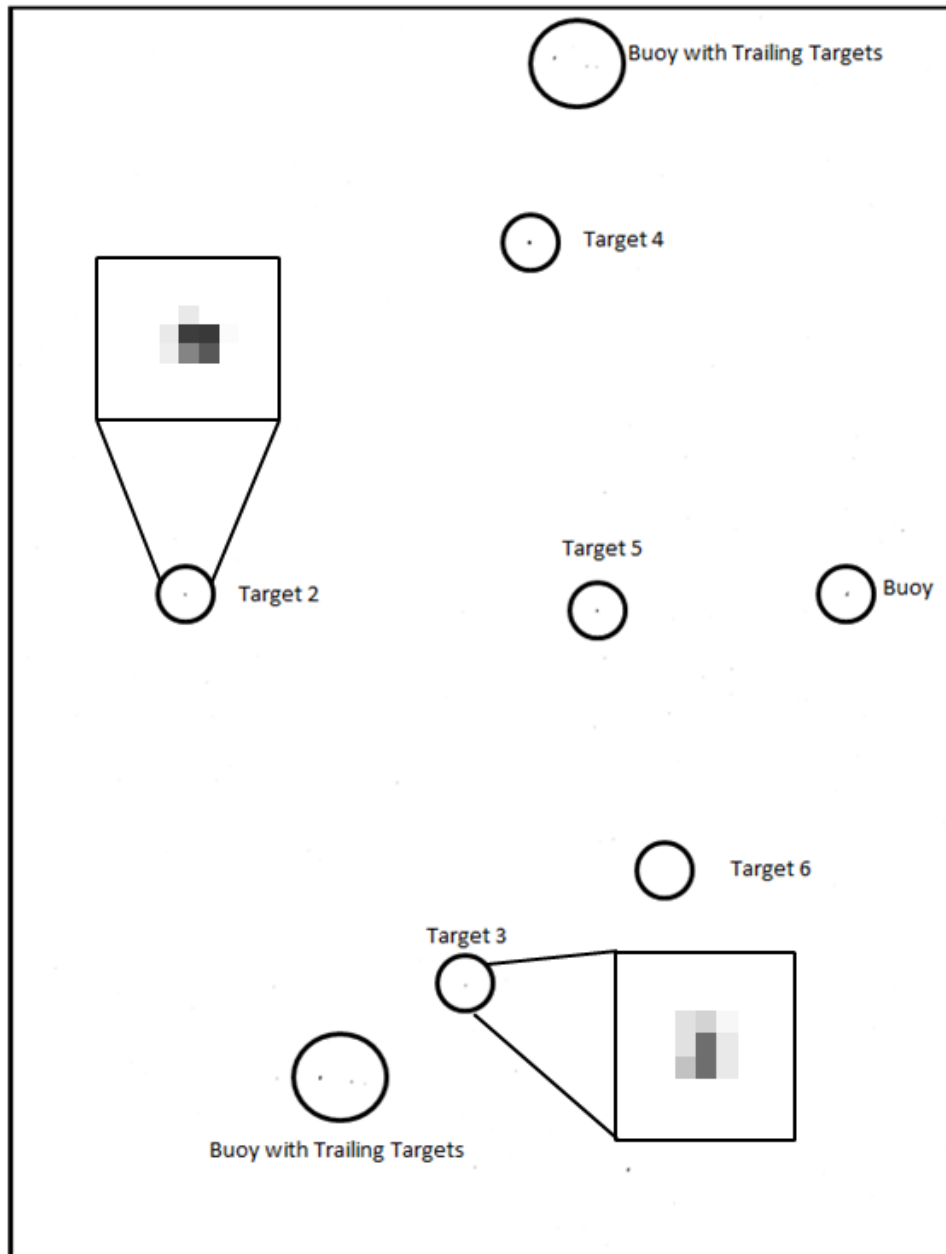
Figure 41.   13 March Histogram Stretch Results: 138 to 196

To come to these results the histogram of the 13 March data was stretched to provide the best representation of the targets. The colors of the resulting image were inverted.

b.   21 March 2012

The stretch for the 21 March data was found to be most favorable between 81 and 231. In this stretch a majority of the targets were observed, with

the exception of targets one, two, and some of the trailing targets. The zodiac is the biggest object in this image. When smoothing was attempted on this image, it eliminated more of the targets from the scene.
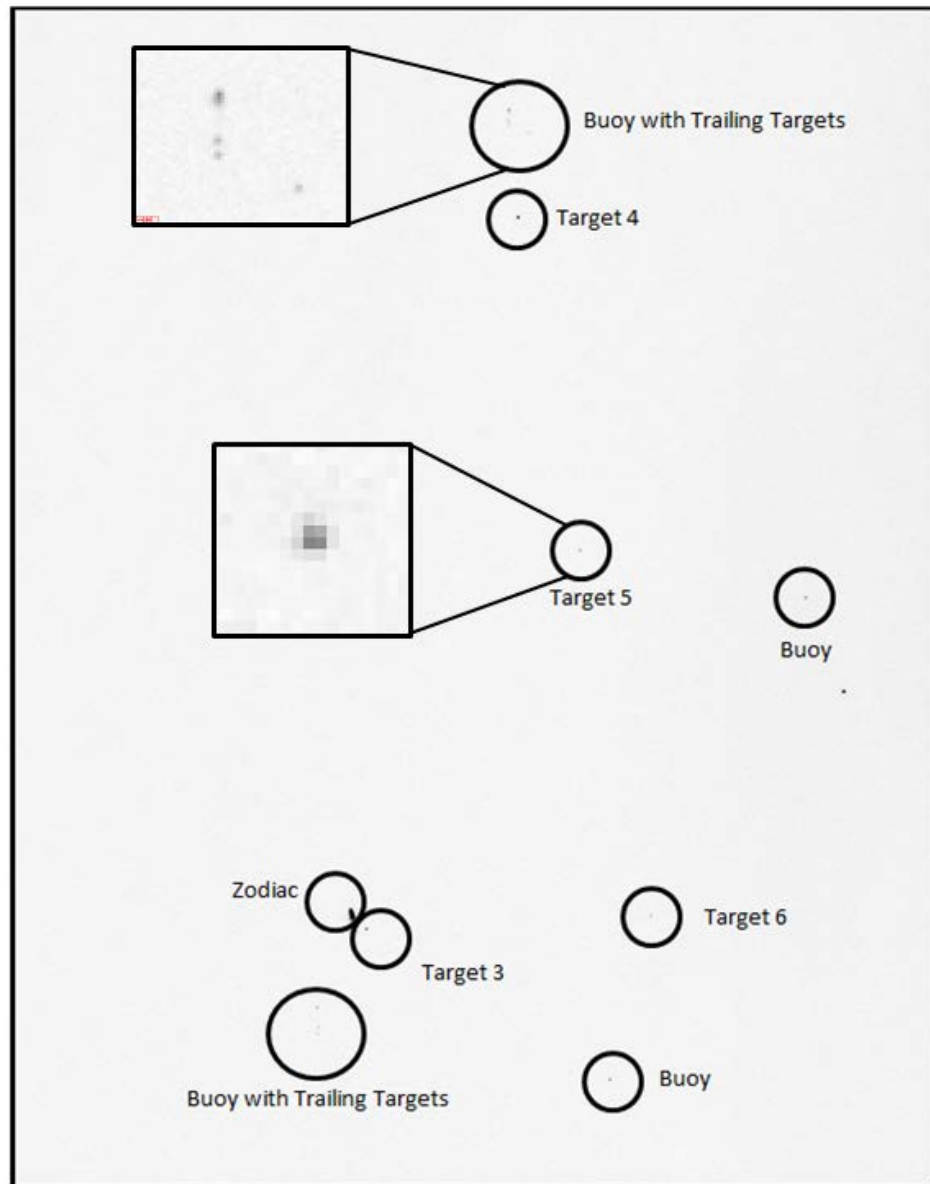

Figure 42.   21 March Histogram Stretch Results: 81-231
The histogram of the 21 March image was stretched between 93 and 889 for this resulting image. Following this method the image colors were inverted.

4. Filters

The default ENVI filters, including both the morphology and convolution, were all applied to the datasets. Once linear stretches were applied targets became apparent. The level of success of this filter varied between the data sets. The filters that were found to be the least useful were: Gaussian high pass, erode, opening and forward FFT. Some of the better results are shown in the following figures. All of the images below except for the directional filter have had their colors inverted for better visibility of targets. In the filters below the targets that were not more than a meter in depth and not dark were successfully picked up by the sensor. One of the submerged targets and the black surface target appear in some of the filters. The targets that were successful at identifying the black target (target six) were the high pass, low pass and directional filters. Target 2 was picked up by the closing, dilate and frost filter. Target one was not discovered in any of the filters. Target five, in particular pixel 9291, 11514, was used to examine the frost filter further. Before the filter was added this pixel had a DN of 188, after the filter the pixels DN was 161. The histogram was created of the DNs and shows that the target does not stand out from the background. Target five is mixed in with the tail of the background, as it also did in the data before the filter was applied. The pixel actually appeared further out on the tail of the histogram in the original dataset.
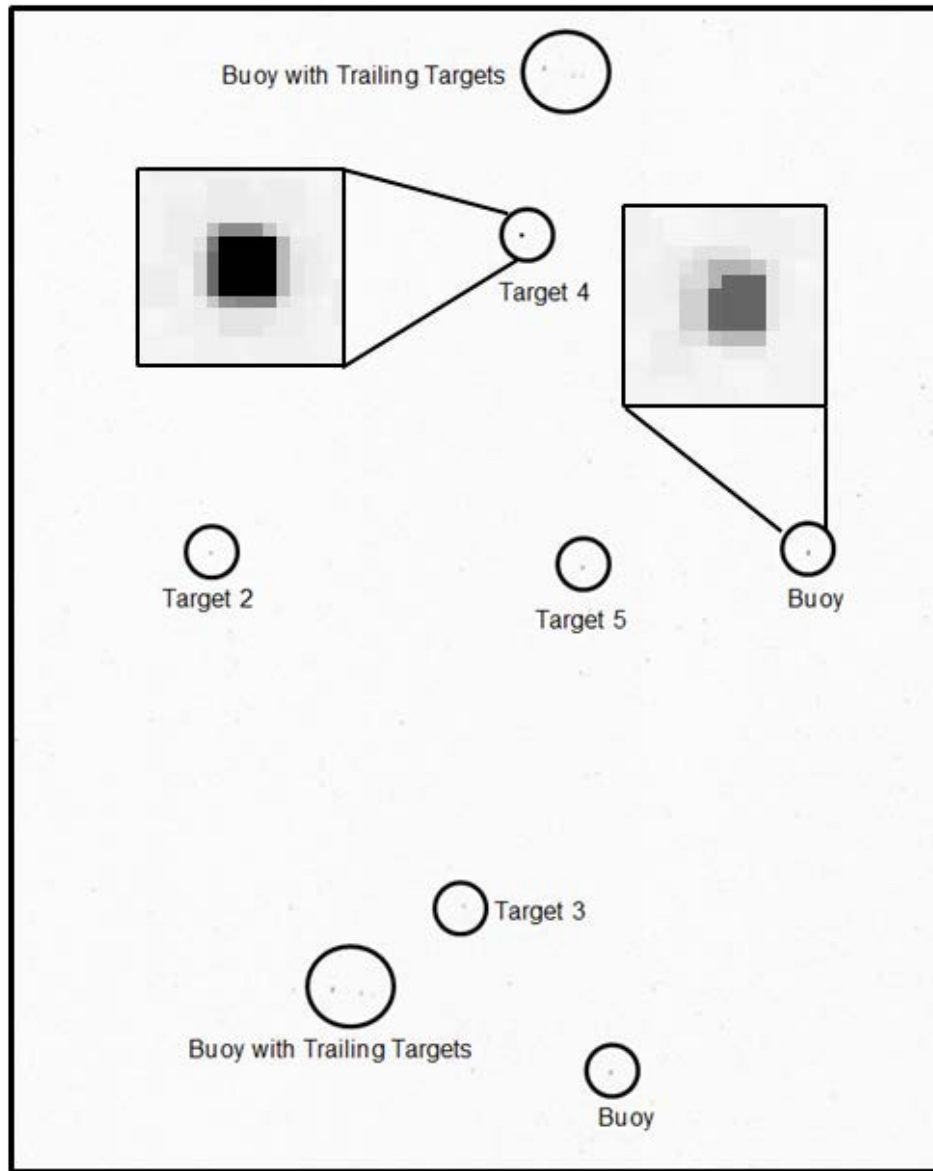
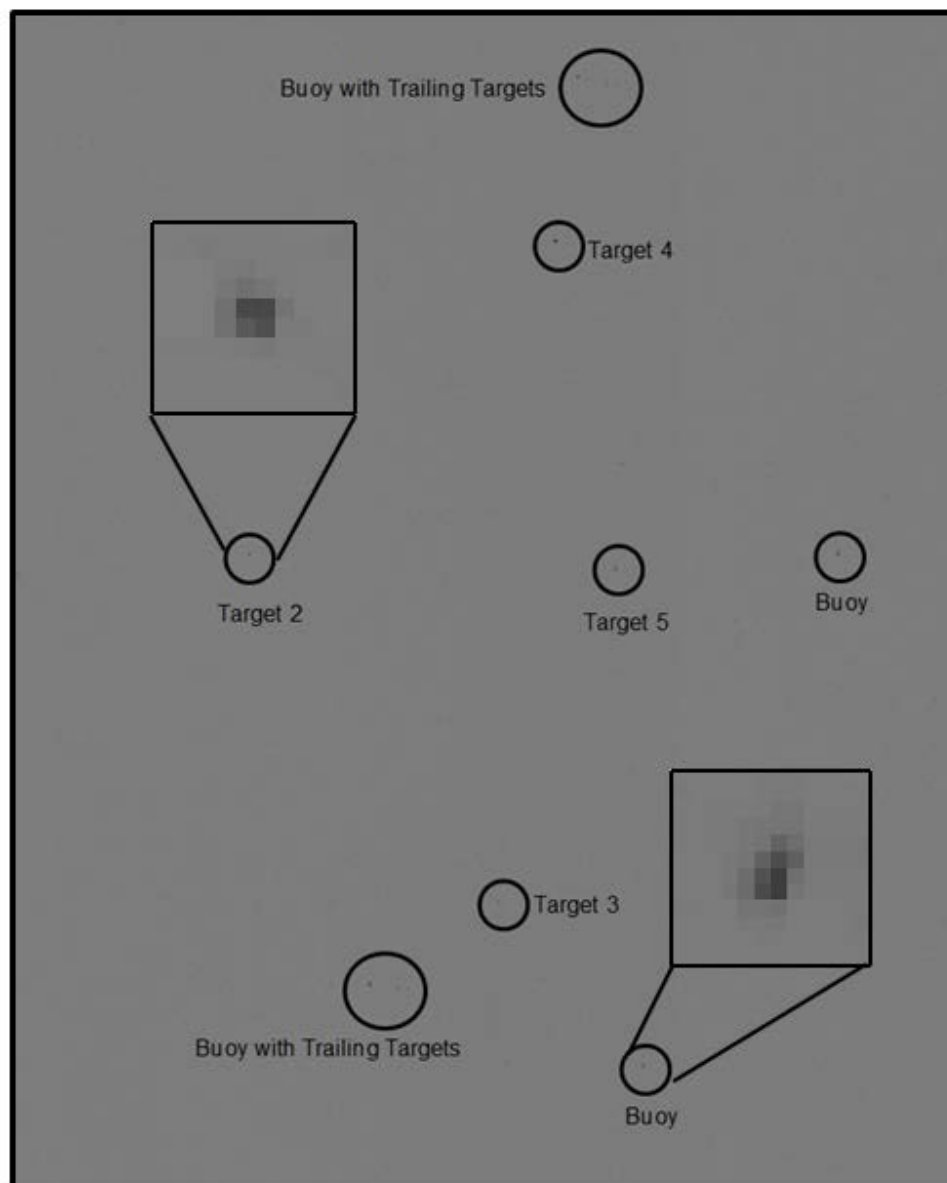Figure 43.   13 March Data, Dilate Filter, Linear Stretch

Figure 44.   13 March Data, Closing Filter, Linear 0-255 Stretch

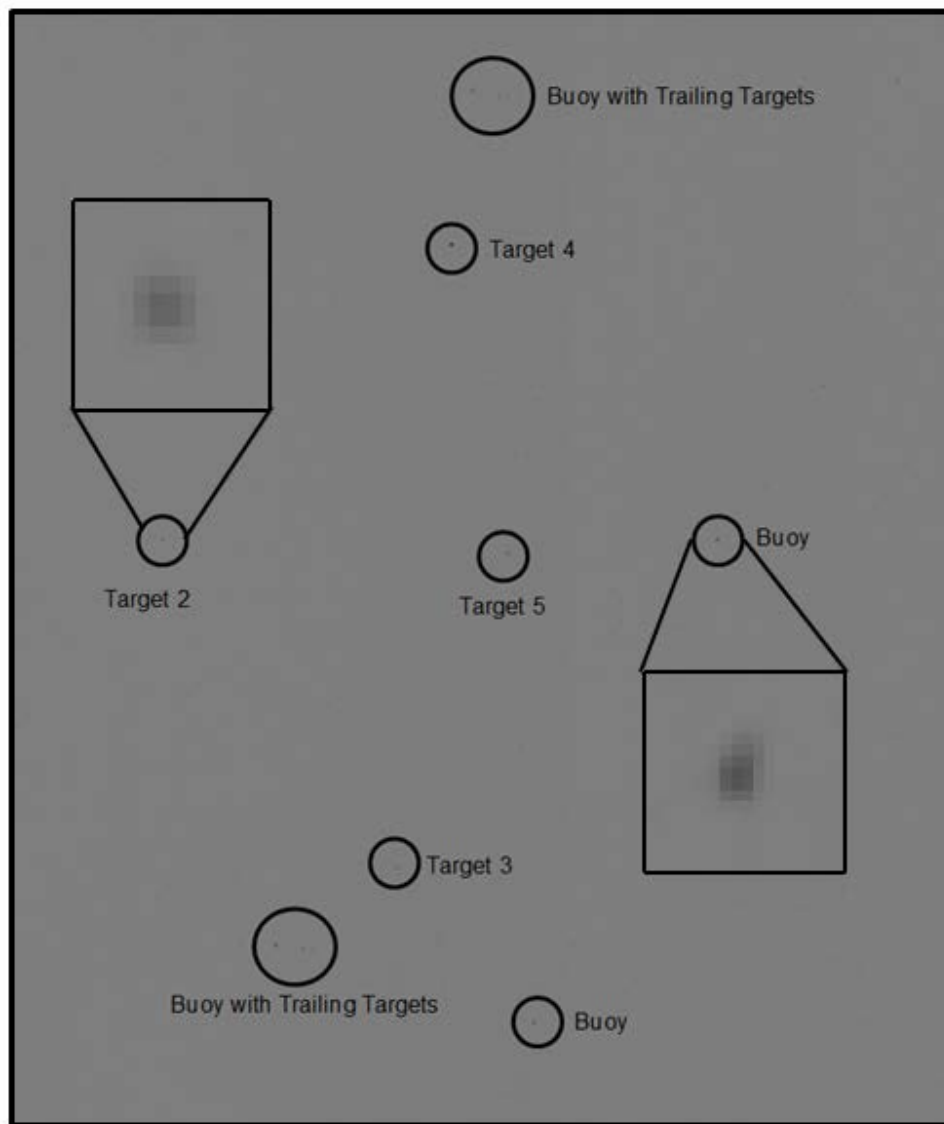Figure 45.   13 March Data, Frost Filter, Linear 0-255 Stretch

Min	0
Max	232
Mean	128.5
Standard deviation	5.94

Table 10.   Statistical results for Frost Filter on Panchromatic 13 March Data Chip

Value Range	Number of Points
201-232	4
151-200	64
136-150	733
131-135	133320
126-130	3620046
101-125	634
1-100	0
0	7784

Table 11.   Pixel Counts of the Frost Filter on the Panchromatic 13 March Data Chip
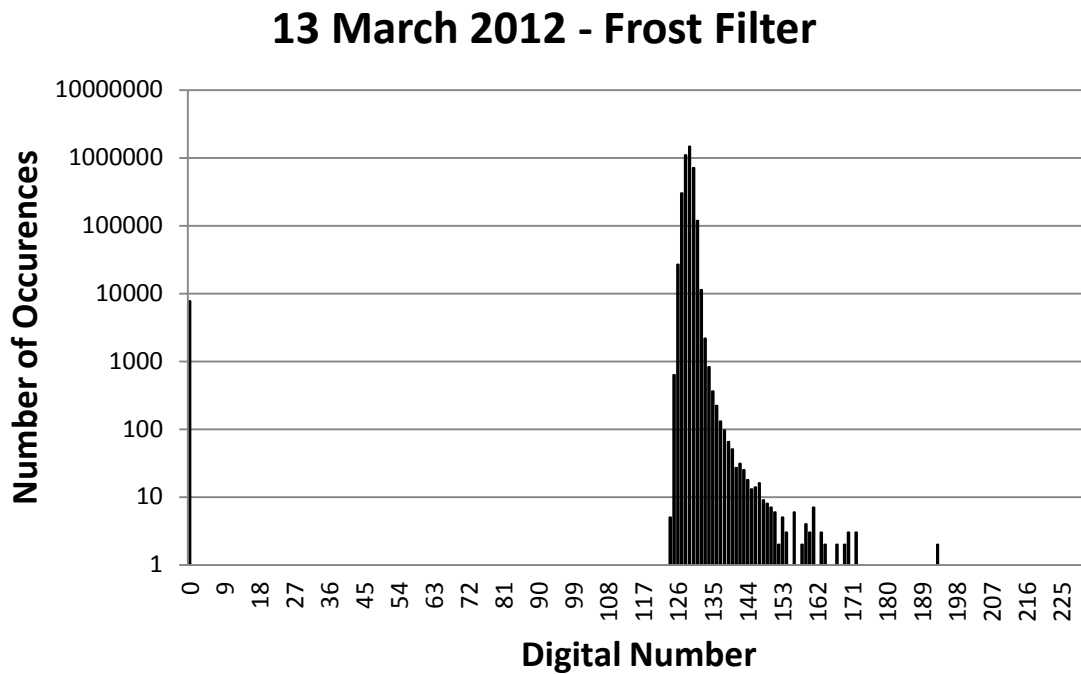
13 March 2012 - Frost Filter

Figure 46.   Histogram of Digital Numbers for Frost Filter on the Panchromatic 13 March Data
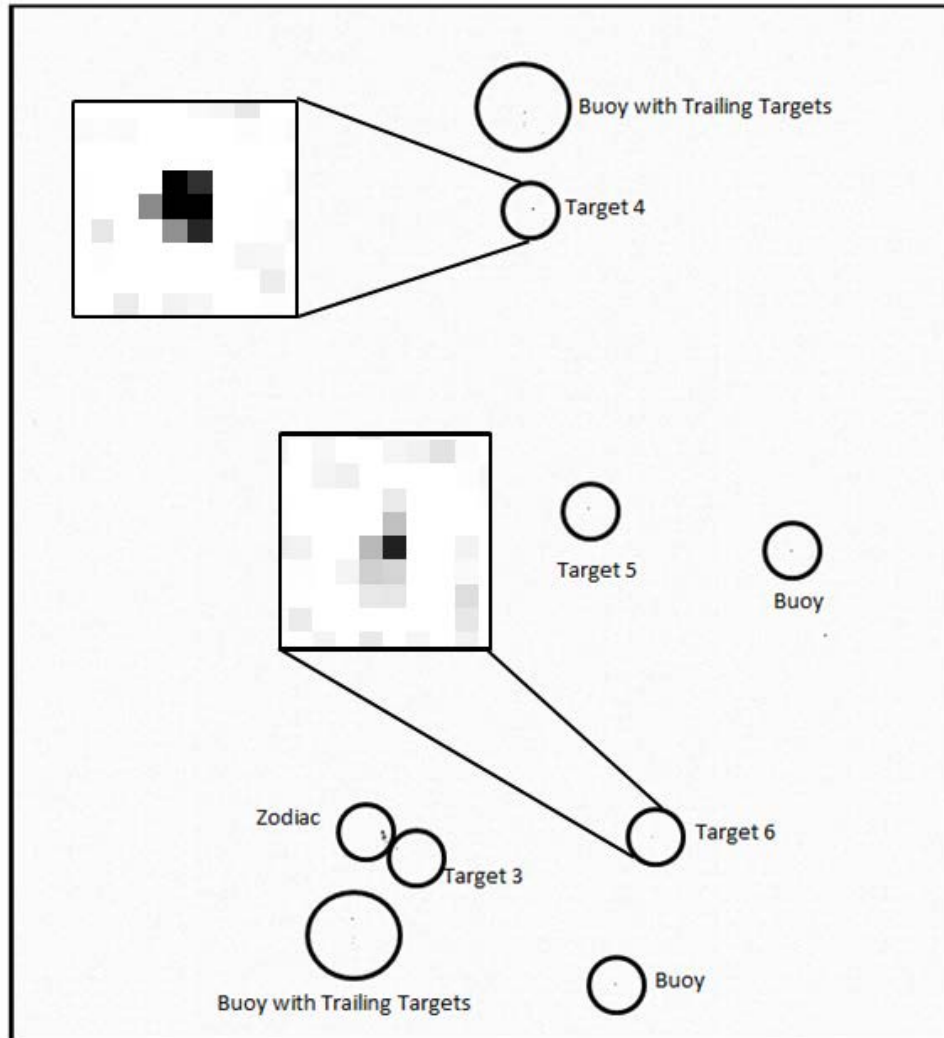
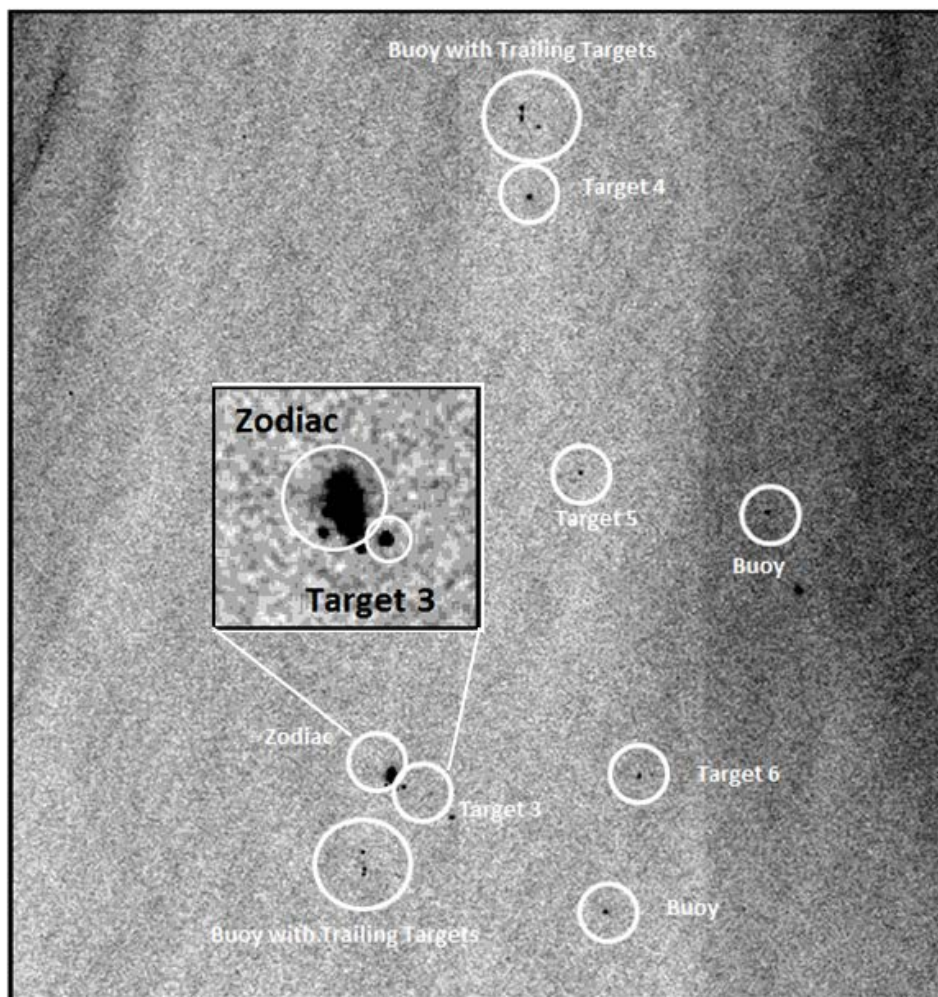Figure 47.   21 March Data, High Pass Filter, Linear 0-255 Stretch

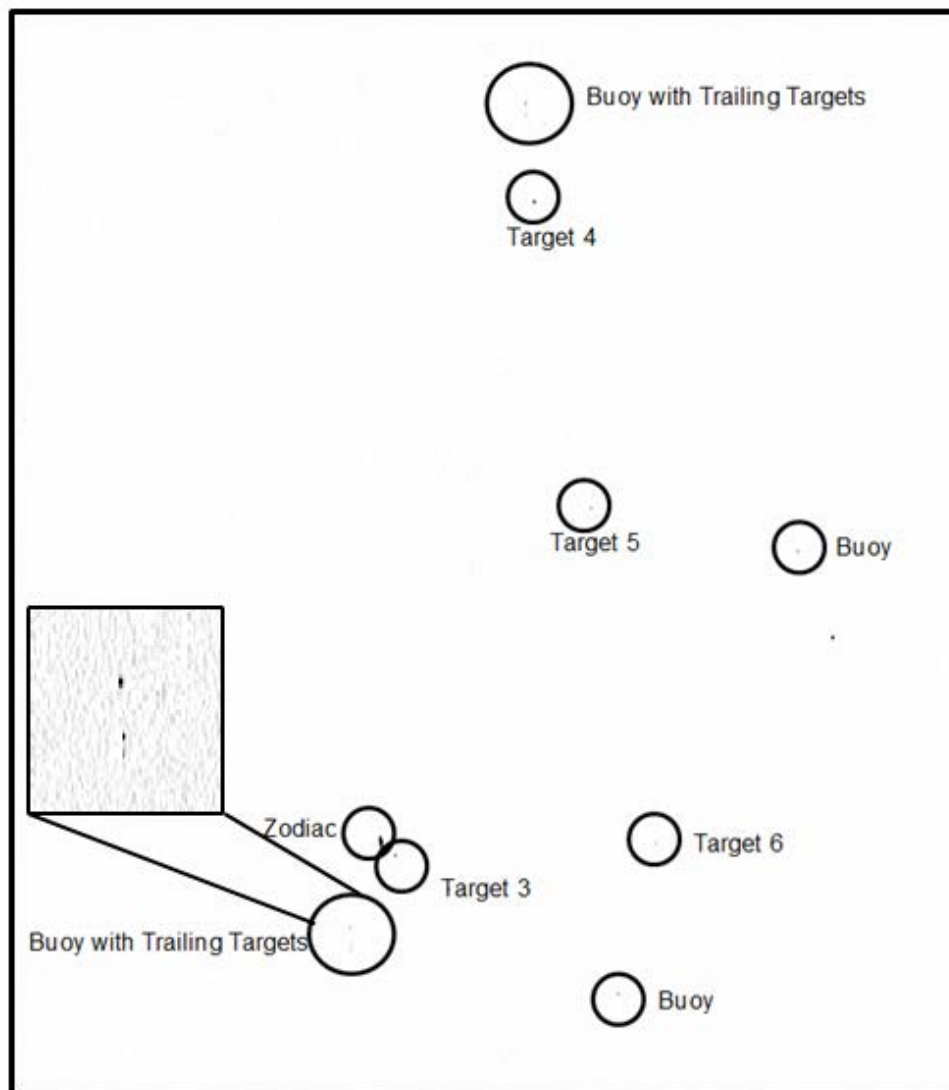Figure 48.　　21 March Data, Low Pass Filter, Linear Stretch

Figure 49.   21 March Data, Directional Filter, Linear 0-255 Stretch

V. CONCLUSIONS

Mine countermeasures is not an easy problem with a single simple solution. While this study determines naval mines can be located using both multispectral and panchromatic methods, it has varying success that is dependent on many different factors. Some of the methods in this paper would not be useful had the location of the targets not have been known. Some of the factors that play a role in the success of locating naval mines include the emissivity of the target's material or the paint covering it, the depth of the mine, the sea state and weather conditions. Varying facts such as the target color and depth played a role in the apparent brightness in the images of this study.

Operationally the goal of a study such as this would be to determine an image processing or analysis technique to find naval mines that does not require many inputs. In mine countermeasures, every situation is going to be different. Some locations or even days will prove to be more difficult than others are when using methods such as those talked about in this paper. One of the reasons for this is clutter in the image. Clutter can be the result of natural features or it can be the results of man-made features on the surface such as vessels. When implementing these methods it is likely, that the data collected will contain vessels that will need to be ruled out as potential naval mines. The zodiac in this study contained a wide variety of values; it also contained pixels with the highest intensity in the scene. Knowing these characteristics of vessels in an image could quickly help rule them out as possible naval mines.

Working with multispectral data with a resolution of two meters has some benefits over higher resolution data. Even though the targets in this study are sub-pixel in size, the fact that they appear in multiple pixels allows them to be more easily noticed. Lower resolution also allows a larger area to be covered in a single image. Multispectral data has files that can be easier to deal with as the file size will be smaller than hyperspectral data.

While it would have been most beneficial to determine a method that would not require much time and effort from a busy analyst, such a multispectral method was not determined from this study. There is not a threshold that will include all the naval mines. The range in the data where the mines are found appears to be different between images.

The PCA method was determined to be the most successful method in this study, as it was the only method that found all the targets. Given that the multispectral had better results than the higher spatial resolution panchromatic it is determined that the spectral characteristics are more critical in this mission. The scatter plot showed that locating these targets relied on both intensity and color. The targets tended to have higher intensity and color then the background. While this method has the best chance of locating naval mines, it is likely it will not have the same high rate of success in all datasets.

If collection conditions are such that large amounts of glint are present in the image, this could have a negative effect on any type of analysis. If the glint cannot successfully be eliminated this can result in high levels of false positives in analysis. Realistically if this was the process being used outside of a test area with known locations, the high level of false positive could lead to much wasted effort and resources of EOD teams attempting to clear naval mines.

With the potential for glint to create such problems analyzing data, a possible alternative would be to use techniques of avoidance with an airborne platform. An airborne platform allows for further control over the collection that is not available with a satellite such as WorldView-2. For instance, WorldView-2 tends to gather all of it data at about 10:30 or 11:00 A.M. local time. While there is possibly the advantage of regular collection and consistency for projects that compare imagery from different days using WorldView-2 methods, this may not be the best choice for this kind of mission. An airborne acquisition campaign allows for better control of imagery collection to better facilitate avoidance methods.

Filters and stretches were used successfully on the panchromatic data; nonetheless, there were still targets that were never detected in the results. The targets that were often left out from the results were the dark or the submerged targets, which are unfortunately, realistic situations for naval mines. When looking at the frost filters it was noted that the DNs of targets actually decreased after the filter was applied, making it more difficult to visually see the target. Based on this the filters may not be the greatest method to peruse when looking for naval mines.

In this study it was found that the targets commonly had pixels with values over 130. While this will not alone provide locations of only naval mines, it could patiently help cue analysts in areas to focus further efforts. Since the DNs of ocean imagery are not consistent, before this is used as practice in theatre more than two images should be examined to determine if this would hold true.

While stretches are normally calculated for the entire image, this does not always have to be the case. Stretches could be based on the zoom window over known target area. This technique could be useful if a target is known and then could be used to find more targets. In this study target one was not detected in any of these analyses, and target two was discovered in the 13 March data but not in the 21 March data. This goes to show that when it comes to mine warfare it can be difficult to find a single solution for finding all naval mines present in a location.

In retrospect there are several ways in which this study could have been improved upon or could be taken further. For instance, it is unrealistic that our adversaries will paint their naval mines bright colors. It would be a more accurate representation if the targets in this study were all dark in color. While this study supports the idea that mine-like targets can be found using the WorldView-2 commercial data. It would be interesting to further this to see how well targets would be depicted in a cluttered environment, since that would be a more realistic situation.

THIS PAGE INTENTIONALLY LEFT BLANK

LIST OF REFERENCES

Allied Joint Force Command Naples. (2012). *NATO mine-hunters sweep approaches to Mistrata harbor*. Retrieved July 10, 2012, from http://www.jfcnaples.nato.int

Ashton, E. A. (1998). Detection of subpixel anomalies in multispectral Infrared Imagery Using an Adaptive Bayesian Classifier. *IEEE Transactions on Geoscience and Remote Sensing*, *36*(2), 506–517.

Ashton, E.A. (1998). Algorithms for the detection of sub-pixel targets in multispectral imagery. *Photogrammetic Engineering & Remote Sensing*, *4*(7), 723–731.

Association of Minemen. (1997). *U.S. Naval Mines And The Minemen: A History*. Dallas: Taylor Publishing Company

Barnes, C., Gilbert, G., Schoonmaker, J., & Rohr, J. (1999). Proceedings of Oceans '99: The possibility of passive whale tracking with the use of a hyperspectral sensor. Seattle, WA: SSC San Diego

Borden, S. A. (2000, April). Mine Countermeasures: A comparative analysis of U.S. Navy mine countermeasures 1999 vs. 2020. Retrieved June 12, 2012, from:http://www.dtic.mil

Burt, C. B. (2012) *Detection of spatially unresolved (nominally subpixel) submerged and surface targets using hyperspectral data*. (Unpublished master's thesis). Naval Postgraduate School, Monterey, CA.

Campbell, J. B. (2007). *Introduction to Remote Sensing* (4th ed.). New York: The Guilford Press.

The Coastal Data Information Program: Integrative Oceanography Division. (2012). Scripts Pier, La Jolla, CA. Retrieved August 29, 2012, from http://cdip.ucsd.edu/

Digital Globe. (2009a). *The benefits of the 8 spectral bands of WorldView-2*. Retrieved March 14, 2012, from: http://worldview2.digitalglobe.com

Digital Globe. (2009b). *About the WorldView-2 satellite.* Retrieved June 6, 2012, from http://worldview2.digitalglobe.com/about

Digital Globe. (2012). *WorldView-2*. Retrieved March 14, 2012, from Digital Globe: http://www.digitalglobe.com/about-us/content-collection#satellites&worldview-2

Elbakary, M.I., & Alam, M.S. (2008). Mine detection in multispectral imagery data using constrained energy minimization. *SPIE*, 6977.

Edwards, A.J. (2012, February). Application of remote sensing to coastal management, part 5: removing sun glint from compact airborne spectrographic imager (CASI) imagery [Bilko Training Modules]. University of Newcastle, U.K.

Gilbert, J.A. (2001, February). *The combined mine countermeasures force: a unified commander-in-chief's answer to the mine threat.* (Report No. AD-A186). Newport, R.I.: Naval War College, Joint Military Operations Department.

Hedley, J. D., Harborne, A. R., & Mumby, P. J. (2005). Simple and robust removal of sun glint for mapping shallow-water benthos. *International Journal of Remote Sensing , 26*(10), 2107–2112.

Holland, K.T., Puleo, J.A., Plant, N., & Kaihatu, J. M. (2002). Littoral environmental nowcasting system (LENS). *IEEE*, 85–91.

Jensen, J. R. (2005). *Introductory Digital Image Processing A Remote Sensing Perspective* (3rd ed). Upper Saddle River: Pearson Prentice Hall.

Jensen, J. R. (2007). *Remote Sensing of the Environment - An Earth Resources Perspective* (2nd ed.). Upper Saddle River: Pearson Prentice Hall.

Joint Chief of Staff. (2010). *Antiterrorism.* Joint Publication 3–07.2. Retrieved March 18, 2012. from http://www.bits.de/NRANEU/others/jp-doctrine/JP3_07.2%2810%29.pdf

Khan, S. (2010). *Iranian mining of the Strait of Hormuz - plausibility and key considerations.* (Special Report No. 4). Institute for Near East & Gulf Military Analysis.

Leonard, C. L., Chan, C. W., Cottis, T., DeWeert, M., Dichner, M., Farm, B. et al. (2008). TACMSI: Anovel multi-look multispectral imager for maritime mine detection. *SPIE*, 6953

Marchisio, G., Pacifici, F., & Padwick, C. (2010). Proceeding of geoscience and remote sensing symposium (IGARSS) 2010: *On the relative predictive value of the new spectral bands in the WorldView-2 sensor.* Honolulu, HI: Digital Globe

Matika, D., Koroman, V. (2001).Chemical and biological medical treatment symposium – Industry II world congress on chemical and biological terrorism, section 35 undersea detection of sea mines. (Report ADA411272). Portland, ME: Applied Science and Analysis Inc.

Mayer, R., & Bucholtz, F. (2003). Object detection by using "whitening/ dewhitening" to transform target signatures in multitemporal and hysperspectral and multispectral imagery. *IEEE*, *41*(5), 1136–1142.

Mobley, C. D. (1994), *Light and Water Radiative Transfer in Natural Waters*. San Diego: Academic Press

Padwick, C., Deskevich, M., Pacifici, F., & Smallwood, S. (2010). Proceedings of ASPRS 2010: *WorldView-2 pan-sharpening*. San Diego, CA: Digital Globe.

Program Executive Office Littoral and Mine Warfare (2009). *21st century U.S. Navy mine warfare - Ensuring Global Access and Commerce.* Retrieved April 4, 2012. from www.navy.mil

Rabiroff, J. (2011, May). U.S. military enters new generatio of sea mine warfare. *Stars and Stripes*. Retrieved Febuary 25, 2012, from http://www.stripes.com/news/u-s-military-enters-new-generation-of-sea-mine-warfare-1.143170

Shirokorad. (2009). Cold-War Era soviet non-contact aviation mines. (Allanea, Trans.).(Original work published 1999). Retrieved July 10, 2012, from http://z4.invisionfree.com/NSDraftroom/ar/t7079.htm

Silva, D., & Ableah, R. (1998). Proceedings for Ocean Optics '98: *Two algorithms for removing ocean surface clutter in multispectral and hyperspectral images*. Kona, HI: SRI International

Theiler, J., & Cai, M. (2003). Resampling approach for anomaly detection in multispectral umages. *SPIE*, 5093, 230–240.

United States Marine Corps. (2009). Amphibious operations in the 21st century. Retrieved April 4, 2012. from http://www.quantico.usmc.mil

Updike, T., & Comp, C. (2010). *Radiometric use of WorldView-2 imagery*. Longmont, CO: Digital Globe

Watts, A. (Ed.). (2005). *Jane's Underwater Warfare Systems 2005–2006*. Alexandria: Jane's Information Group Inc.

Whitford, M. (2005, April). GPS guides autonomous underwater vehicles. *GPS World.* Retrieved July 10, 2012, from http://www.gpsworld.com

THIS PAGE INTENTIONALLY LEFT BLANK

INITIAL DISTRIBUTION LIST

1. Defense Technical Information Center
    Ft. Belvoir, Virginia

2. Dudley Knox Library
    Naval Postgraduate School
    Monterey, California

3. Dr. Richard C. Olsen
    Naval Postgraduate School
    Monterey, California

4. Dr. Charlene Sailer
    Naval Postgraduate School
    Monterey, California

5. Dr. Dan C. Boger
    Naval Postgraduate School
    Monterey, California

6. Maj. Neal Hinson
    Headquarters Air Force A2
    Washington, D.C.

7. Maj. Joshua Smith
    Beale Air Force Base
    Beale Air Force Base, California

8. Kevin Whitcomb
    UTC Aerospace Systems
    Westford, MA